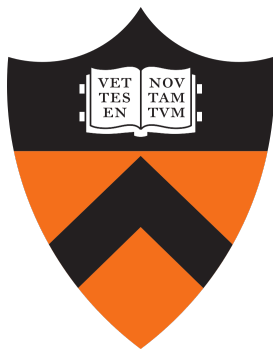


DYNAMICAL STABILITY OF BINARY PLANETS IN COMPACT
MULTI-PLANETARY SYSTEMS



WOLF Z. CUKIER

ADVISED BY TANSU DAYLAN

SECOND READER BY ROMAIN TEYSSIER

A PAPER SUBMITTED IN PARTIAL FULFILLMENT OF THE
REQUIREMENTS FOR THE CERTIFICATE IN APPLIED AND
COMPUTATIONAL MATHEMATICS

PRINCETON UNIVERSITY

SPRING 2024

Abstract

We have built a model to evaluate the potential dynamical stability of binary planets in compact multi-planetary systems. We have identified 49 candidate systems that we then simulated in 3 scenarios—No Injection where we simulate the system including only known bodies, Single Injection where we simulate the system with the addition of an additional planet, and Binary Injection where we simulate the system with the addition of a pair of binary planets. We have noticed that a large number of the existing solutions for planetary systems are unstable and likely could be better constrained with further dynamical modeling. We have also identified 6 systems for further study as they have high stability of either additional single planets (4 systems) or moderate stability of additional binary planet pairs (3 systems).

1 Introduction

Binary planets, also known as double planets, are pairs of planets that orbit each other, making a shared orbit around their star. Although no known binary planets exist, the closest solar system analogues are the Earth-Moon and Pluto-Charon systems. These systems have a more complex orbital geometry than the usual single planets, which mean that they may be able to evade detection by the usual detection techniques for planets. The transit method of detecting planets, which detects planets via the light blocked as they pass between the star and our telescope, relies on strictly periodic orbits in a strictly defined orbital plane for automated algorithms to identify the weak signals caused by transits as originating from planets. Binary planets may not transit periodically, even as other planets in the system do so, as the inclination of the binary planets' orbit around each other may cause planets to be out of the orbital plane of the system at time of transit, causing the transit to not occur. Additionally, as the planets' orbit around each other has a distinct period to the planets' orbit around their host star, the planets will be at different

orbital phases at time of transit, breaking the periodicity required for common transit detection algorithms to actually find a planet.

One common feature of known exoplanetary systems is that many of them are compact. Many systems have a large number of planets located incredibly close to their star—Famously, the TRAPPIST-1 system has 7 planets contained within a fraction of Mercury’s orbit. A number of these systems have “dynamical-gaps” or regions that given the spacing of the other planets in the system, we would expect to find a planet. My project focuses on these systems, compact-multiplanetary systems with a dynamical gap and seeks to determine if the existence of a binary planet within the system would explain the gap.

2 Methodology

2.1 Determination of Sample Planets

We began by identifying a list of known exoplanetary-systems that are compact-multiplanetary systems with enough known properties such that we can effectively study them. We filtered the list of ~ 4000 known exoplanetary systems as of June 2023 taken from the Exoplanet Archive¹ to include systems with at least 4 planets with semi-major axis less than 1 au and which have for which there exists transit data in the default solution provided by Exoplanet Archive. The 49 systems which meet our filtering criteria are displayed in Figure 1.

2.2 Simulation Priors

We then performed a Monte-Carlo simulation to determine the stability of the exoplanetary systems. We initialized each system by drawing from our priors for each system. We determined our priors for the stellar mass, and the planetary mass, semi-major

¹<https://exoplanetarchive.ipac.caltech.edu/>

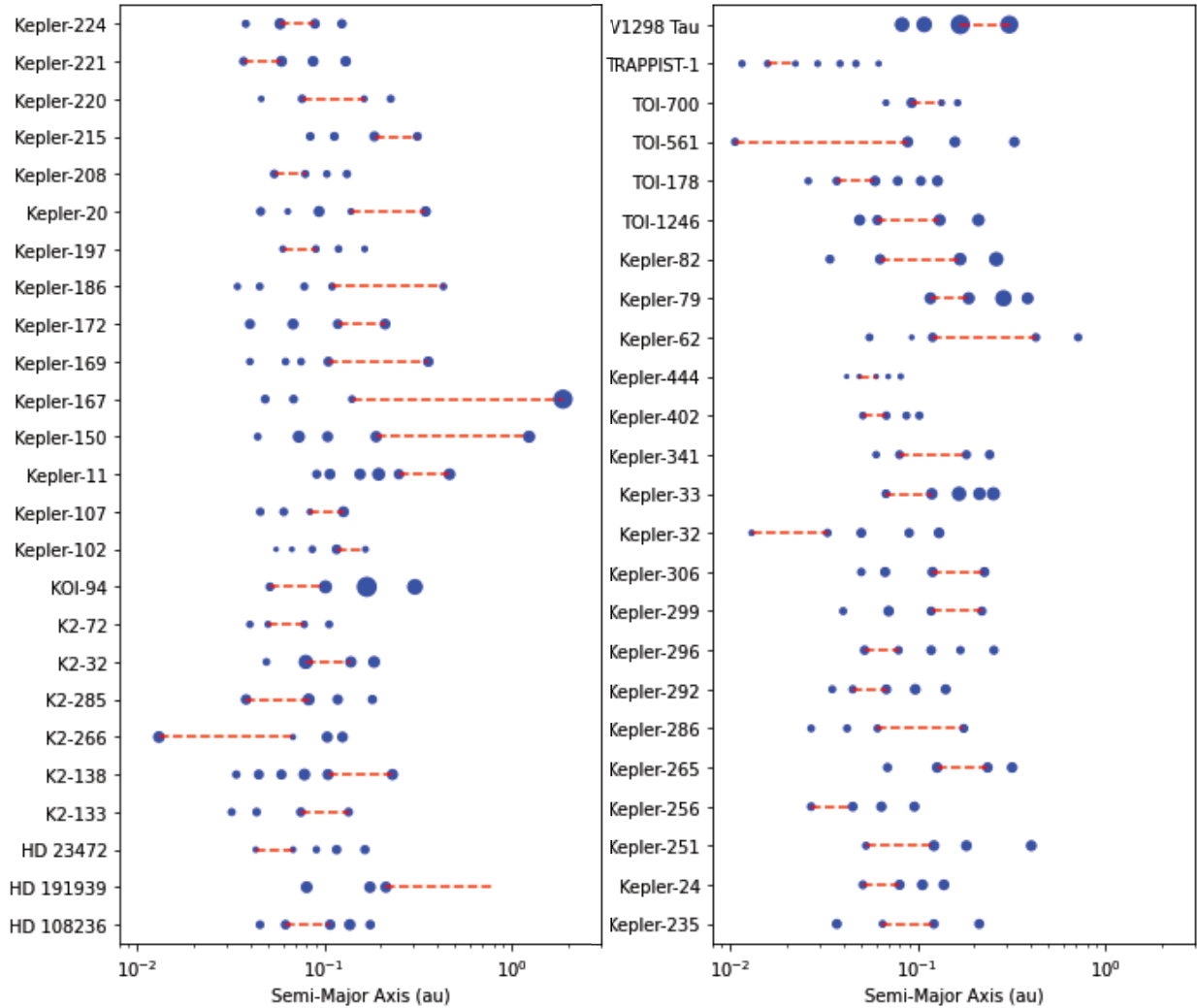


Figure 1: The selected planetary systems considered in this study. The blue dots represent the location of the planets, the size of the dots correlates with the radius of the planets, and the red dashed line represents the dynamical gap of the system.

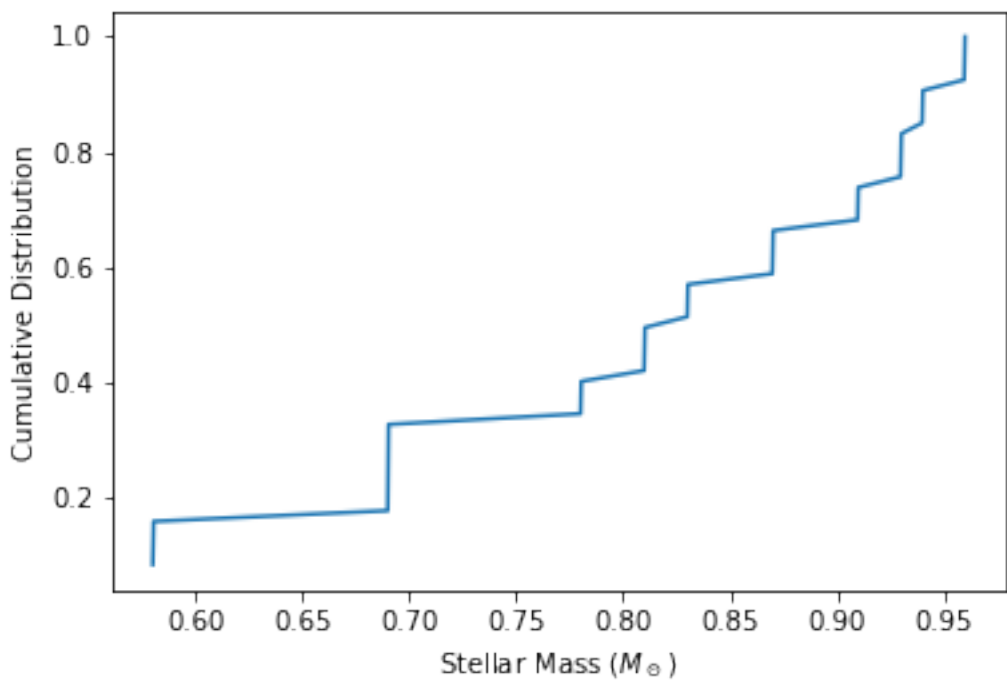


Figure 2: Empirical cumulative probability distribution used for determining stellar masses given no published priors.

axis, and eccentricity by pulling data from the default solution on the Exoplanet Archive.

If constraints on these variables existed, we took our prior to be a uniform distribution between the $\pm 1\sigma$ bounds. We additionally set the inclination of each planet to be 0.

If the host star of the system did not have complete mass constraints with a most likely mass and $\pm 1\sigma$ bounds, we determined the stellar mass by drawing from an empirical mass distribution that was created from the stars with constrained masses in our sample. This distribution is presented in Figure 2. We note that this mass distribution is slightly out of date and does not include all eligible stars from our present sample. Likewise, if a planet did not have complete mass constraints we set the mass using mass-radius relations. If an upper mass bound existed, we used rejection sampling of the mass-radius relation to determine the mass subject to that upper bound. If no complete eccentricity data was available, we took the eccentricity to be 0. By our selection criteria, a most likely semi-major axis exists for each planet in our sample. If either the error lower bound or the error upper bound did not exist, we assumed it to be 80% and 120% respectively of the most likely semi-major axis. We did likewise if the error bounds were missing for radius on a planet that we were using mass-radius relationships to determine their mass.

Mass-Radius relationships were determined by using the `forecaster` python module developed by Chen and Kipping (2017). System specific stellar mass priors for each system are presented in 4. Likewise our priors for planetary mass, semi-major axis, eccentricity, and, if applicable, radius are presented in 5. The applicable citations for the data used are also presented in the aforementioned tables.

We ran three scenarios for each system—A No Injection case where we simulate only the known planets, a Single Injection case where we simulate the known planets with the addition of a single planet in the largest dynamical gap, and a Binary Injection case where we simulate the known planets along with the addition of a binary planet pair in the largest dynamical gap. As we expect the planets to be roughly evenly spaced in

logarithmic space, we determined the largest dynamical gap by taking the ratio:

$$r_i = \frac{a_{i+1}}{a_i} \quad (1)$$

for each pair of planets where a_i is the semi-major axis of the $i - th$ planet in the system. The region corresponding with the maximum value of r_i is considered the dynamical gap and the locations of such gaps are noted in Figure 1.

For the single injection case, we took the prior distribution of the mass of the injected planet to be a normal distribution with the mean and standard deviation taken from the mean and standard deviation of the set of known planets, which previously had their masses determined by the method as discussed above. We additionally set the semi-major axis of the planet to be a uniform distribution over the region

$$G = (a_j + 0.2(a_{j+1} - a_j), a_j + 0.8(a_{j+1} - a_j)) \ni r_j = \max_i(\{r_i\}). \quad (2)$$

We set the eccentricity to be a uniform distribution over the interval $(0, 0.3)$ as we found that planets with eccentricity $e > 0.3$ had negligible rates of survival. The inclination of the injected planet was set to 0. A summary of these priors is presented in Table 2.

For the binary injection case we parameterized the masses of the two planets in terms of the total mass of the binary system, m_{tot} , and in terms of the mass fraction of the smaller planet, q . The masses of the planets, (m_1, m_2) , were then set as

$$(m_1, m_2) = (qm_{\text{tot}}, (1 - q)m_{\text{tot}}). \quad (3)$$

The prior on the total system mass was a uniform prior on the interval $(0.38M_{\oplus}, 72M_{\oplus})$ which was chosen to approximately cover the mass range of planets in the 49 systems. The mass fraction of the smaller planet was chosen to be uniform on the interval $(0.25, 0.5)$ so we allow the larger planet to be anywhere from the same mass as the smaller planet to 4

times more massive. The eccentricity of the planets about their center of mass, e , and the eccentricity of the center of mass about the star, e_{sys} was drawn from a uniform distribution on the interval $(0, 0.3)$. The semi-major axis of the center of mass around the star was drawn a uniform distribution on the interval given in Equation 2. The distance between the planets, d , which is equal to twice the semi-major axis about the center of mass, was drawn from a uniform distribution on the interval $(0.1r_{\text{Hill}}, 0.8r_{\text{Hill}})$ where r_{Hill} is the hill radius of the more massive planet and is given by

$$r_{\text{Hill}} = a_{\text{sys}}(1 - e) \left(\frac{m_2}{3M_{\text{star}}} \right)^{1/3}. \quad (4)$$

Both the orbit of the planets around the center of mass of the binary system and of the center of mass around the host star had their inclinations set to zero. The phase of the planets in their orbit around each other was uniformly randomized. A summary of these priors is presented in Table 3.

2.3 N-Body Simulation

We then simulated each initialized system in a N-body simulation using the `rebound` python package (Rein and Liu, 2012). We performed performance and accuracy tests on all the built in integrators in `rebound`, the results of which are presented in Table 1, and chose to use the `leapfrog` integrator due to its speed and accuracy. The `leapfrog` integrator is a relatively simple second order symplectic integrator that is implemented in a drift-kick-drift scheme. The Hamiltonian for a particle with mass m ,

$$H = \frac{1}{2} \frac{p^2}{m} + \Phi(x) \quad (5)$$

where $\Phi(x)$ is the gravitational potential, is split into two components $H_1(p) = \frac{1}{2} \frac{p^2}{m}$ and $H_2(x) = \Phi(x)$ such that $H = H_1 + H_2$. The co-ordinates of a particle with momentum and

position at timestep i , (p_i, x_i) , are time evolved as follows:

$$x_{i+1/2} = \left. \frac{\partial H_1}{\partial p} \right|_i \frac{\Delta t}{2} = \frac{p_i}{m} \frac{\Delta t}{2} \quad (6)$$

$$p_{i+1} = - \left. \frac{\partial H_2}{\partial x} \right|_{i+1/2} \Delta t = -\nabla \phi(x_{i+1/2}) \Delta t \quad (7)$$

$$x_{i+1} = \left. \frac{\partial H_1}{\partial p} \right|_{i+1} \frac{\Delta t}{2} = \frac{p_{i+1}}{m} \frac{\Delta t}{2} \quad (8)$$

As the leapfrog integrator is a symplectic error, it is guaranteed to preserve quantities such as angular momentum and energy.

Each run was performed for 1,000,000 years at a time step of $\Delta t = 0.0001$ years. The simulation was stopped early and considered unstable if any planet became gravitationally unbound or was on an orbit with semi-major axis $a > 5$ au. Systems that ran to completion were considered stable if the final semi-major axes of every planet were within 10% of their starting values.

For each system and each scenario pair, we performed a maximum of 10000 runs by running our simulation on 96 cores for 4 hours. The minimum amount of runs achieved by this method was ~ 600 . The runs per system is significantly lower for systems that are more stable as the early stopping allows for unstable systems to quickly explore the unstable parts of the parameter space.

3 Results

We begin by presenting summary results for the three scenarios. A histogram describing how stable the various systems we simulated in each scenario are is presented in Figure 3. Greater 65% of the systems in the No Injection scenario were stable in over 10% of runs, with many systems being more stable than that threshold, but over 20% of the No Injection systems were unstable over 99% of the time. We have yet to break down the

| Integrator | Time (s) | Energy Error | Angular Momentum Error |
|------------|----------|------------------------|------------------------|
| EOS | 291 | 8.55×10^{-11} | 2.47×10^{-8} |
| SEI | 167 | 3.23 | 4.83×10^{11} |
| Leapfrog | 125 | 9.77×10^{-11} | 2.89×10^{-7} |
| SABA | 2443 | 8.91×10^{-11} | 4.18×10^{-6} |
| Janus | 846 | 5.56×10^{-13} | 4.38×10^{-8} |
| IAS15 | 294 | 1.37×10^{-15} | 6.78×10^{-8} |
| Mercurius | long | N/A | N/A |
| WHfast | 430 | 1.23×10^{-10} | 1.09×10^{-7} |
| BS | 27 | 2.21×10^{-6} | 5.75×10^{-2} |
| TES | 230 | 2.31×10^{-14} | 1.22×10^{-9} |

Table 1: Comparison of run-time and error of the `rebound` built in integrators. Note that the Mercurius integrator timed out so we do not know its exact runtime.

| Quantity | Prior |
|-----------------|---|
| Mass | $\text{Normal}(\text{mean}(m_{\text{planets}}), \text{std}(m_{\text{planets}})),$ |
| Semi-Major Axis | $U(G)$ |
| Eccentricity | $U(0, 0.3)$ |
| Inclination | $\pi/2$ |

Table 2: Priors for the single injected planet. Note that the interval G is given in Equation 2.

| Quantity | Prior |
|-----------------------|---------------------------------------|
| Total Mass | $U(0.38, 0.72) M_{\oplus},$ |
| Mass-Fraction (q) | $U(0.25, 0.5)$ |
| Semi-Major Axis | $U(G)$ |
| Eccentricity | $U(0, 0.3)$ |
| System Eccentricity | $U(0, 0.3)$ |
| Inclination | 0 |
| Planet Separation | Uniform(0.1, 0.8) * r_{Hill} |

Table 3: Priors for the binary injected planets. Note that the interval G is given in Equation 2 and the Equation for the Hill radius, r_{Hill} is given in Equation 4.

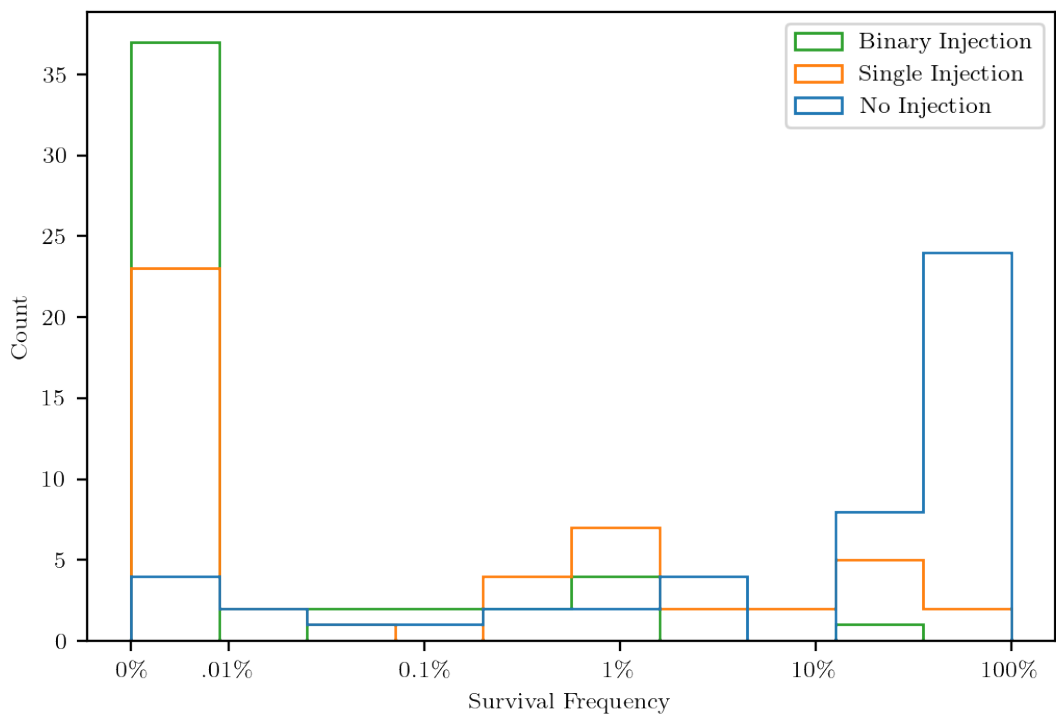


Figure 3: Histogram of survival frequency, or the fraction of runs that were considered dynamically stable, for the three injection scenarios.

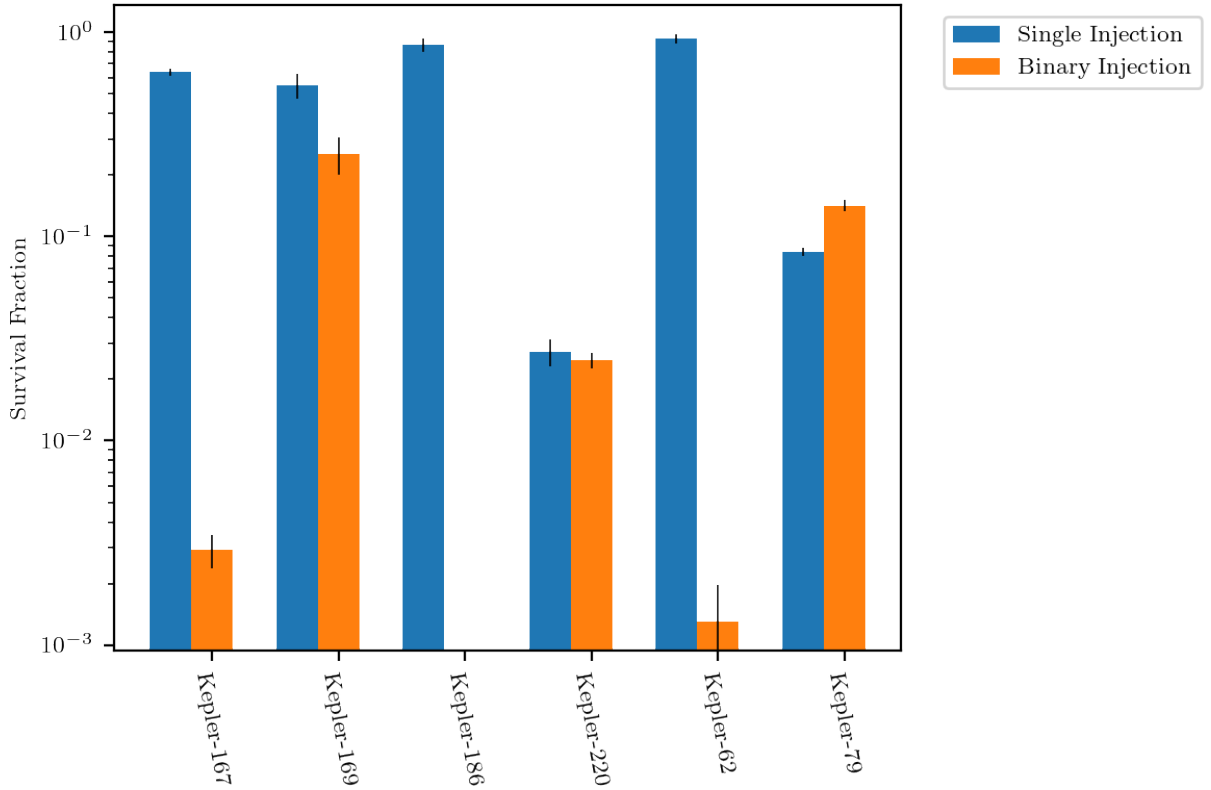


Figure 4: Survival fractions for six selected planetary systems for the Single and Binary Injection Scenarios, normalized to the survival fraction of the No Injection Scenario. Error bars represent $\pm\sigma$ using Poisson statistics.

fraction of these systems that had unconstrained priors that we had to estimate, but the lack of stability in the vast majority of cases indicates that dynamical modeling that takes into account dynamical stability could likely be useful in further constraining the orbital and bulk parameters of these systems.

As expected, adding in extra planets in the single injection case significantly decreased the likelihood of stability. In the Single Injection scenario just under 50% of the systems are stable while for the Binary Injection case the vast majority (75%) of systems fail to ever achieve stability in all of their runs. $\sim 15\%$ of the Single Injection systems and one of the Binary Injection systems, however, are stable at least 10% of the time.

A selection of the 6 most interesting systems is presented in Figure 4. These are systems

where the Single Injection scenario had a survival rate of at least half that of the No Injection scenario or where the Binary Injection Scenario had a survival rate of at least 1%. The systems Kepler-167, Kepler-169, Kepler-186, and Kepler-62 are interesting as they all have high survival rates of Single Injection at or above 50% of the No Injection scenario. These are systems where the dynamics do not appear to preclude the existence of additional planets in the dynamical gap and thus might be interesting candidates for follow-up searches.

The Kepler-220, Kepler-169, and Kepler-79 systems, and especially the latter two, are also interesting due to the relative high stability rate of the binary planets. All of these systems have binary planet survival rates greater than 10% with the survival rate in Kepler-79 for binary planets actually being greater than that for single injection. The dynamical gaps of these systems, likewise, would be a good location to search for potential binary planets.

Acknowledgments

I would like to thank Tansu for graciously serving as my advisor for this project even though I probably had to cancel every third meeting with nowhere enough notice. I would also like to thank the denizens of the Noether Nook and The Cafe for their continued support and friendship throughout this time working on the project.

This paper represents my work in accordance with University regulations.

/s/ Wolf Cukier

Software

- `numpy` (Harris et al., 2020)
- `matplotlib` (Hunter, 2007)
- `rebound` (Rein and Liu, 2012)
- `scipy` (Virtanen et al., 2020)
- `forecaster` (Chen and Kipping, 2016)

References

- Agol, E., Dorn, C., Grimm, S. L., Turbet, M., Ducrot, E., Delrez, L., Gillon, M., Demory, B.-O., Burdanov, A., Barkaoui, K., Benkhaldoun, Z., Bolmont, E., Burgasser, A., Carey, S., de Wit, J., Fabrycky, D., Foreman-Mackey, D., Haldemann, J., Hernandez, D. M., Ingalls, J., Jehin, E., Langford, Z., Leconte, J., Lederer, S. M., Luger, R., Malhotra, R., Meadows, V. S., Morris, B. M., Pozuelos, F. J., Queloz, D., Raymond, S. N., Selsis, F., Sestovic, M., Triaud, A. H. M. J., and Van Grootel, V. (2021). Refining the Transit-timing and Photometric Analysis of TRAPPIST-1: Masses, Radii, Densities, Dynamics, and Ephemerides. *The Planetary Science Journal*, 2:1. Publisher: IOP ADS Bibcode: 2021PSJ.....2....1A.
- Barclay, T., Quintana, E. V., Adams, F. C., Ciardi, D. R., Huber, D., Foreman-Mackey, D., Montet, B. T., and Caldwell, D. (2015). The Five Planets in the Kepler-296 Binary System All Orbit the Primary: A Statistical and Analytical Analysis. *The Astrophysical Journal*, 809:7. Publisher: IOP ADS Bibcode: 2015ApJ...809....7B.
- Barros, S. C. C., Demangeon, O. D. S., Alibert, Y., Leleu, A., Adibekyan, V., Lovis, C., Bossini, D., Sousa, S. G., Hara, N., Bouchy, F., Lavie, B., Rodrigues, J., Gomes da Silva, J., Lillo-Box, J., Pepe, F. A., Tabernero, H. M., Zapatero Osorio, M. R., Sozzetti, A., Suárez Mascareño, A., Micela, G., Allende Prieto, C., Cristiani, S., Damasso, M., Di Marcantonio, P., Ehrenreich, D., Faria, J., Figueira, P., González Hernández, J. I., Jenkins, J., Lo Curto, G., Martins, C. J. A. P., Micela, G., Nunes, N. J., Pallé, E., Santos, N. C., Rebolo, R., Seager, S., Twicken, J. D., Udry, S., Vanderspek, R., and Winn, J. N. (2022). HD 23472: a multi-planetary system with three super-Earths and two potential super-Mercuries. *Astronomy and Astrophysics*, 665:A154. ADS Bibcode: 2022A&A...665A.154B.
- Bonfanti, A., Delrez, L., Hooton, M. J., Wilson, T. G., Fossati, L., Alibert, Y., Hoyer, S.,

Mustill, A. J., Osborn, H. P., Adibekyan, V., Gandolfi, D., Salmon, S., Sousa, S. G., Tuson, A., Van Grootel, V., Cabrera, J., Nascimbeni, V., Maxted, P. F. L., Barros, S. C. C., Billot, N., Bonfils, X., Borsato, L., Broeg, C., Davies, M. B., Deleuil, M., Demangeon, O. D. S., Fridlund, M., Lacedelli, G., Lendl, M., Persson, C., Santos, N. C., Scandariato, G., Szabó, G. M., Collier Cameron, A., Udry, S., Benz, W., Beck, M., Ehrenreich, D., Fortier, A., Isaak, K. G., Queloz, D., Alonso, R., Asquier, J., Bandy, T., Bárczy, T., Barrado, D., Barragán, O., Baumjohann, W., Beck, T., Bekkelien, A., Bergomi, M., Brandeker, A., Busch, M. D., Cessa, V., Charnoz, S., Chazelas, B., Corral Van Damme, C., Demory, B. O., Erikson, A., Farinato, J., Futyana, D., Garcia Muñoz, A., Gillon, M., Guedel, M., Guterman, P., Hasiba, J., Heng, K., Hernandez, E., Kiss, L., Kuntzer, T., Laskar, J., Lecavelier des Etangs, A., Lovis, C., Magrin, D., Malvacio, L., Marafatto, L., Michaelis, H., Munari, M., Olofsson, G., Ottacher, H., Ottensamer, R., Pagano, I., Pallé, E., Peter, G., Piazza, D., Piotto, G., Pollacco, D., Ragazzoni, R., Rando, N., Ratti, F., Rauer, H., Ribas, I., Rieder, M., Rohlfs, R., Safa, F., Salatti, M., Ségransan, D., Simon, A. E., Smith, A. M. S., Sordet, M., Steller, M., Thomas, N., Tschentscher, M., Van Eylen, V., Viotto, V., Walter, I., Walton, N. A., Wildi, F., and Wolter, D. (2021). CHEOPS observations of the HD 108236 planetary system: a fifth planet, improved ephemerides, and planetary radii. *Astronomy and Astrophysics*, 646:A157. ADS Bibcode: 2021A&A...646A.157B.

Bonomo, A. S., Dumusque, X., Massa, A., Mortier, A., Bongiolatti, R., Malavolta, L., Sozzetti, A., Buchhave, L. A., Damasso, M., Haywood, R. D., Morbidelli, A., Latham, D. W., Molinari, E., Pepe, F., Poretti, E., Udry, S., Affer, L., Boschin, W., Charbonneau, D., Cosentino, R., Cretignier, M., Ghedina, A., Lega, E., López-Morales, M., Margini, M., Martínez Fiorenzano, A. F., Mayor, M., Micela, G., Pedani, M., Pinamonti, M., Rice, K., Sasselov, D., Tronsgaard, R., and Vanderburg, A. (2023). Cold Jupiters and improved masses in 38 Kepler and K2 small planet systems from 3661 HARPS-N radial velocities. No excess of cold Jupiters in small planet systems. *Astronomy and Astrophysics*, 677:A33. ADS Bibcode: 2023A&A...677A..33B.

Borucki, W. J., Agol, E., Fressin, F., Kaltenegger, L., Rowe, J., Isaacson, H., Fischer, D., Batalha, N., Lissauer, J. J., Marcy, G. W., Fabrycky, D., Désert, J.-M., Bryson, S. T., Barclay, T., Bastien, F., Boss, A., Brugamyer, E., Buchhave, L. A., Burke, C., Caldwell, D. A., Carter, J., Charbonneau, D., Crepp, J. R., Christensen-Dalsgaard, J., Christiansen, J. L., Ciardi, D., Cochran, W. D., DeVore, E., Doyle, L., Dupree, A. K., Endl, M., Everett, M. E., Ford, E. B., Fortney, J., Gautier, T. N., Geary, J. C., Gould, A., Haas, M., Henze, C., Howard, A. W., Howell, S. B., Huber, D., Jenkins, J. M.,

Kjeldsen, H., Kolbl, R., Kolodziejczak, J., Latham, D. W., Lee, B. L., Lopez, E., Mullally, F., Orosz, J. A., Prsa, A., Quintana, E. V., Sanchis-Ojeda, R., Sasselov, D., Seader, S., Shporer, A., Steffen, J. H., Still, M., Tenenbaum, P., Thompson, S. E., Torres, G., Twicken, J. D., Welsh, W. F., and Winn, J. N. (2013). Kepler-62: A Five-Planet System with Planets of 1.4 and 1.6 Earth Radii in the Habitable Zone. *Science*, 340:587–590. ADS Bibcode: 2013Sci...340..587B.

Campante, T. L., Barclay, T., Swift, J. J., Huber, D., Adibekyan, V. Z., Cochran, W., Burke, C. J., Isaacson, H., Quintana, E. V., Davies, G. R., Silva Aguirre, V., Ragozzine, D., Riddle, R., Baranec, C., Basu, S., Chaplin, W. J., Christensen-Dalsgaard, J., Metcalfe, T. S., Bedding, T. R., Handberg, R., Stello, D., Brewer, J. M., Hekker, S., Karoff, C., Kolbl, R., Law, N. M., Lundkvist, M., Miglio, A., Rowe, J. F., Santos, N. C., Van Laerhoven, C., Arentoft, T., Elsworth, Y. P., Fischer, D. A., Kawaler, S. D., Kjeldsen, H., Lund, M. N., Marcy, G. W., Sousa, S. G., Sozzetti, A., and White, T. R. (2015). An Ancient Extrasolar System with Five Sub-Earth-size Planets. *The Astrophysical Journal*, 799:170. Publisher: IOP ADS Bibcode: 2015ApJ...799..170C.

Chachan, Y., Dalba, P. A., Knutson, H. A., Fulton, B. J., Thorngren, D., Beichman, C., Ciardi, D. R., Howard, A. W., and Van Zandt, J. (2022). Kepler-167e as a Probe of the Formation Histories of Cold Giants with Inner Super-Earths. *The Astrophysical Journal*, 926:62. Publisher: IOP ADS Bibcode: 2022ApJ...926..62C.

Chen, J. and Kipping, D. (2016). PROBABILISTIC FORECASTING OF THE MASSES AND RADII OF OTHER WORLDS. *The Astrophysical Journal*, 834(1):17.

Chen, J. and Kipping, D. M. (2017). Probabilistic Forecasting of the Masses and Radii of Other Worlds. *The Astrophysical Journal*, 834(1):17. arXiv:1603.08614 [astro-ph].

David, T. J., Petigura, E. A., Luger, R., Foreman-Mackey, D., Livingston, J. H., Mamajek, E. E., and Hillenbrand, L. A. (2019). Four Newborn Planets Transiting the Young Solar Analog V1298 Tau. *The Astrophysical Journal*, 885:L12. Publisher: IOP ADS Bibcode: 2019ApJ...885L..12D.

Dressing, C. D., Vanderburg, A., Schlieder, J. E., Crossfield, I. J. M., Knutson, H. A., Newton, E. R., Ciardi, D. R., Fulton, B. J., Gonzales, E. J., Howard, A. W., Isaacson, H., Livingston, J., Petigura, E. A., Sinukoff, E., Everett, M., Horch, E., and Howell, S. B. (2017). Characterizing K2 Candidate Planetary Systems Orbiting Low-mass Stars. II. Planetary Systems Observed During Campaigns 1-7. *The Astronomical Journal*, 154:207. Publisher: IOP ADS Bibcode: 2017AJ....154..207D.

Fabrycky, D. C., Ford, E. B., Steffen, J. H., Rowe, J. F., Carter, J. A., Moorhead, A. V., Batalha, N. M., Borucki, W. J., Bryson, S., Buchhave, L. A., Christiansen, J. L., Ciardi, D. R., Cochran, W. D., Endl, M., Fanelli, M. N., Fischer, D., Fressin, F., Geary, J., Haas, M. R., Hall, J. R., Holman, M. J., Jenkins, J. M., Koch, D. G., Latham, D. W., Li, J., Lissauer, J. J., Lucas, P., Marcy, G. W., Mazeh, T., McCauliff, S., Quinn, S., Ragozzine, D., Sasselov, D., and Shporer, A. (2012). Transit Timing Observations from Kepler. IV. Confirmation of Four Multiple-planet Systems by Simple Physical Models. *The Astrophysical Journal*, 750:114. Publisher: IOP ADS Bibcode: 2012ApJ...750..114F.

Ford, E. B., Fabrycky, D. C., Steffen, J. H., Carter, J. A., Fressin, F., Holman, M. J., Lissauer, J. J., Moorhead, A. V., Morehead, R. C., Ragozzine, D., Rowe, J. F., Welsh, W. F., Allen, C., Batalha, N. M., Borucki, W. J., Bryson, S. T., Buchhave, L. A., Burke, C. J., Caldwell, D. A., Charbonneau, D., Clarke, B. D., Cochran, W. D., Désert, J.-M., Endl, M., Everett, M. E., Fischer, D. A., Gautier, III, T. N., Gilliland, R. L., Jenkins, J. M., Haas, M. R., Horch, E., Howell, S. B., Ibrahim, K. A., Isaacson, H., Koch, D. G., Latham, D. W., Li, J., Lucas, P., MacQueen, P. J., Marcy, G. W., McCauliff, S., Mullally, F. R., Quinn, S. N., Quintana, E., Shporer, A., Still, M., Tenenbaum, P., Thompson, S. E., Torres, G., Twicken, J. D., Wohler, B., and Kepler Science Team (2012). Transit Timing Observations from Kepler. II. Confirmation of Two Multiplanet Systems via a Non-parametric Correlation Analysis. *The Astrophysical Journal*, 750:113. Publisher: IOP ADS Bibcode: 2012ApJ...750..113F.

Freudenthal, J., von Essen, C., Ofir, A., Dreizler, S., Agol, E., Wedemeyer, S., Morris, B. M., Becker, A. C., Deeg, H. J., Hoyer, S., Mallonn, M., Poppenhaeger, K., Herrero, E., Ribas, I., Boumis, P., and Liakos, A. (2019). Kepler Object of Interest Network. III. Kepler-82f: a new non-transiting 21 M planet from photodynamical modelling. *Astronomy and Astrophysics*, 628:A108. ADS Bibcode: 2019A&A...628A.108F.

Gilbert, E. A., Vanderburg, A., Rodriguez, J. E., Hord, B. J., Clement, M. S., Barclay, T., Quintana, E. V., Schlieder, J. E., Kane, S. R., Jenkins, J. M., Twicken, J. D., Kunimoto, M., Vanderspek, R., Arney, G. N., Charbonneau, D., Günther, M. N., Huang, C. X., Isopi, G., Kostov, V. B., Kristiansen, M. H., Latham, D. W., Mallia, F., Mamajek, E. E., Mireles, I., Quinn, S. N., Ricker, G. R., Schulte, J., Seager, S., Suissa, G., Winn, J. N., Youngblood, A., and Zapparata, A. (2023). A Second Earth-sized Planet in the Habitable Zone of the M Dwarf, TOI-700. *The Astrophysical Journal*, 944:L35. Publisher: IOP ADS Bibcode: 2023ApJ...944L..35G.

Harris, C. R., Millman, K. J., van der Walt, S. J., Gommers, R., Virtanen, P., Cournapeau,

- D., Wieser, E., Taylor, J., Berg, S., Smith, N. J., Kern, R., Picus, M., Hoyer, S., van Kerkwijk, M. H., Brett, M., Haldane, A., del Río, J. F., Wiebe, M., Peterson, P., Gérard-Marchant, P., Sheppard, K., Reddy, T., Weckesser, W., Abbasi, H., Gohlke, C., and Oliphant, T. E. (2020). Array programming with NumPy. *Nature*, 585(7825):357–362. Number: 7825 Publisher: Nature Publishing Group.
- Hunter, J. D. (2007). Matplotlib: A 2D Graphics Environment. *Computing in Science & Engineering*, 9(3):90–95.
- Jontof-Hutter, D., Lissauer, J. J., Rowe, J. F., and Fabrycky, D. C. (2014). Kepler-79’s Low Density Planets. *The Astrophysical Journal*, 785:15. Publisher: IOP ADS Bibcode: 2014ApJ...785...15J.
- Lacedelli, G., Wilson, T. G., Malavolta, L., Hooton, M. J., Collier Cameron, A., Alibert, Y., Mortier, A., Bonfanti, A., Haywood, R. D., Hoyer, S., Piotto, G., Bekkelien, A., Vanderburg, A. M., Benz, W., Dumusque, X., Deline, A., López-Morales, M., Borsato, L., Rice, K., Fossati, L., Latham, D. W., Brandeker, A., Poretti, E., Sousa, S. G., Sozzetti, A., Salmon, S., Burke, C. J., Van Grootel, V., Fausnaugh, M. M., Adibekyan, V., Huang, C. X., Osborn, H. P., Mustill, A. J., Pallé, E., Bourrier, V., Nascimbeni, V., Alonso, R., Anglada, G., Bárczy, T., Barrado y Navascues, D., Barros, S. C. C., Baumjohann, W., Beck, M., Beck, T., Billot, N., Bonfils, X., Broeg, C., Buchhave, L. A., Cabrera, J., Charnoz, S., Cosentino, R., Csizmadia, S., Davies, M. B., Deleuil, M., Delrez, L., Demangeon, O., Demory, B. O., Ehrenreich, D., Erikson, A., Esparza-Borges, E., Florén, H. G., Fortier, A., Fridlund, M., Futyan, D., Gandolfi, D., Ghedina, A., Gillon, M., Güdel, M., Guterman, P., Harutyunyan, A., Heng, K., Isaak, K. G., Jenkins, J. M., Kiss, L., Laskar, J., Lecavelier des Etangs, A., Lendl, M., Lovis, C., Magrin, D., Marafatto, L., Martinez Fiorenzano, A. F., Maxted, P. F. L., Mayor, M., Micela, G., Molinari, E., Murgas, F., Narita, N., Olofsson, G., Ottensamer, R., Pagano, I., Pasetti, A., Pedani, M., Pepe, F. A., Peter, G., Phillips, D. F., Pollacco, D., Queloz, D., Ragazzoni, R., Rando, N., Ratti, F., Rauer, H., Ribas, I., Santos, N. C., Sasselov, D., Scandariato, G., Seager, S., Ségransan, D., Serrano, L. M., Simon, A. E., Smith, A. M. S., Steinberger, M., Steller, M., Szabó, G., Thomas, N., Twicken, J. D., Udry, S., Walton, N., and Winn, J. N. (2022). Investigating the architecture and internal structure of the TOI-561 system planets with CHEOPS, HARPS-N, and TESS. *Monthly Notices of the Royal Astronomical Society*, 511:4551–4571. Publisher: OUP ADS Bibcode: 2022MNRAS.511.4551L.
- Leleu, A., Alibert, Y., Hara, N. C., Hooton, M. J., Wilson, T. G., Robutel, P., Delisle,

J. B., Laskar, J., Hoyer, S., Lovis, C., Bryant, E. M., Ducrot, E., Cabrera, J., Delrez, L., Acton, J. S., Adibekyan, V., Allart, R., Allende Prieto, C., Alonso, R., Alves, D., Anderson, D. R., Angerhausen, D., Anglada Escudé, G., Asquier, J., Barrado, D., Barros, S. C. C., Baumjohann, W., Bayliss, D., Beck, M., Beck, T., Bekkelien, A., Benz, W., Billot, N., Bonfanti, A., Bonfils, X., Bouchy, F., Bourrier, V., Boué, G., Brandeker, A., Broeg, C., Buder, M., Burdanov, A., Burleigh, M. R., Bárczy, T., Cameron, A. C., Chamberlain, S., Charnoz, S., Cooke, B. F., Corral Van Damme, C., Correia, A. C. M., Cristiani, S., Damasso, M., Davies, M. B., Deleuil, M., Demangeon, O. D. S., Demory, B. O., Di Marcantonio, P., Di Persio, G., Dumusque, X., Ehrenreich, D., Erikson, A., Figueira, P., Fortier, A., Fossati, L., Fridlund, M., Futyana, D., Gandolfi, D., García Muñoz, A., Garcia, L. J., Gill, S., Gillen, E., Gillon, M., Goad, M. R., González Hernández, J. I., Guedel, M., Günther, M. N., Haldemann, J., Henderson, B., Heng, K., Hogan, A. E., Isaak, K., Jehin, E., Jenkins, J. S., Jordán, A., Kiss, L., Kristiansen, M. H., Lam, K., Lavie, B., Lecavelier des Etangs, A., Lendl, M., Lillo-Box, J., Lo Curto, G., Magrin, D., Martins, C. J. A. P., Maxted, P. F. L., McCormac, J., Mehner, A., Micela, G., Molero, P., Moyano, M., Murray, C. A., Nascimbeni, V., Nunes, N. J., Olofsson, G., Osborn, H. P., Oshagh, M., Ottensamer, R., Pagano, I., Pallé, E., Pedersen, P. P., Pepe, F. A., Persson, C. M., Peter, G., Piotto, G., Polenta, G., Pollacco, D., Poretti, E., Pozuelos, F. J., Queloz, D., Ragazzoni, R., Rando, N., Ratti, F., Rauer, H., Raynard, L., Rebolo, R., Reimers, C., Ribas, I., Santos, N. C., Scandariato, G., Schneider, J., Sebastian, D., Sestovic, M., Simon, A. E., Smith, A. M. S., Sousa, S. G., Sozzetti, A., Steller, M., Suárez Mascareño, A., Szabó, G. M., Ségransan, D., Thomas, N., Thompson, S., Tilbrook, R. H., Triaud, A., Turner, O., Udry, S., Van Grootel, V., Venus, H., Verrecchia, F., Vines, J. I., Walton, N. A., West, R. G., Wheatley, P. J., Wolter, D., and Zapatero Osorio, M. R. (2021). Six transiting planets and a chain of Laplace resonances in TOI-178. *Astronomy and Astrophysics*, 649:A26. ADS Bibcode: 2021A&A...649A..26L.

Lillo-Box, J., Lopez, T. A., Santerne, A., Nielsen, L. D., Barros, S. C. C., Deleuil, M., Acuña, L., Mousis, O., Sousa, S. G., Adibekyan, V., Armstrong, D. J., Barrado, D., Bayliss, D., Brown, D. J. A., Demangeon, O. D. S., Dumusque, X., Figueira, P., Hojjatpanah, S., Osborn, H. P., Santos, N. C., and Udry, S. (2020). Masses for the seven planets in K2-32 and K2-233. Four diverse planets in resonant chain and the first young rocky worlds. *Astronomy and Astrophysics*, 640:A48. ADS Bibcode: 2020A&A...640A..48L.

Lissauer, J. J., Jontof-Hutter, D., Rowe, J. F., Fabrycky, D. C., Lopez, E. D., Agol, E.,

Marcy, G. W., Deck, K. M., Fischer, D. A., Fortney, J. J., Howell, S. B., Isaacson, H., Jenkins, J. M., Kolbl, R., Sasselov, D., Short, D. R., and Welsh, W. F. (2013). All Six Planets Known to Orbit Kepler-11 Have Low Densities. *The Astrophysical Journal*, 770:131. Publisher: IOP ADS Bibcode: 2013ApJ...770..131L.

Lissauer, J. J., Marcy, G. W., Rowe, J. F., Bryson, S. T., Adams, E., Buchhave, L. A., Ciardi, D. R., Cochran, W. D., Fabrycky, D. C., Ford, E. B., Fressin, F., Geary, J., Gilliland, R. L., Holman, M. J., Howell, S. B., Jenkins, J. M., Kinemuchi, K., Koch, D. G., Morehead, R. C., Ragozzine, D., Seader, S. E., Tanenbaum, P. G., Torres, G., and Twicken, J. D. (2012). Almost All of Kepler's Multiple-planet Candidates Are Planets. *The Astrophysical Journal*, 750:112. Publisher: IOP ADS Bibcode: 2012ApJ...750..112L.

Lopez, T. A., Barros, S. C. C., Santerne, A., Deleuil, M., Adibekyan, V., Almenara, J. M., Armstrong, D. J., Brugger, B., Barrado, D., Bayliss, D., Boisse, I., Bonomo, A. S., Bouchy, F., Brown, D. J. A., Carli, E., Demangeon, O., Dumusque, X., Díaz, R. F., Faria, J. P., Figueira, P., Foxell, E., Giles, H., Hébrard, G., Hojjatpanah, S., Kirk, J., Lillo-Box, J., Lovis, C., Mousis, O., da Nóbrega, H. J., Nielsen, L. D., Neal, J. J., Osborn, H. P., Pepe, F., Pollacco, D., Santos, N. C., Sousa, S. G., Udry, S., Vigan, A., and Wheatley, P. J. (2019). Exoplanet characterisation in the longest known resonant chain: the K2-138 system seen by HARPS. *Astronomy and Astrophysics*, 631:A90. ADS Bibcode: 2019A&A...631A..90L.

Lubin, J., Van Zandt, J., Holcomb, R., Weiss, L. M., Petigura, E. A., Robertson, P., Akana Murphy, J. M., Scarsdale, N., Batygin, K., Polanski, A. S., Batalha, N. M., Crossfield, I. J. M., Dressing, C., Fulton, B., Howard, A. W., Huber, D., Isaacson, H., Kane, S. R., Roy, A., Beard, C., Blunt, S., Chontos, A., Dai, F., Dalba, P. A., Gary, K., Giacalone, S., Hill, M. L., Mayo, A., Močnik, T., Kosiarek, M. R., Rice, M., Rubenzahl, R. A., Latham, D. W., Seager, S., Winn, J. N., and Gary, K. (2022). TESS-Keck Survey. IX. Masses of Three Sub-Neptunes Orbiting HD 191939 and the Discovery of a Warm Jovian plus a Distant Substellar Companion. *The Astronomical Journal*, 163:101. Publisher: IOP ADS Bibcode: 2022AJ....163..101L.

Orell-Miquel, J., Nowak, G., Murgas, F., Palle, E., Morello, G., Luque, R., Badenas-Agusti, M., Ribas, I., Lafarga, M., Espinoza, N., Morales, J. C., Zechmeister, M., Alqasim, A., Cochran, W. D., Gandolfi, D., Goffo, E., Kabáth, P., Korth, J., Lam, K. W. F., Livingston, J., Muresan, A., Persson, C. M., and Van Eylen, V. (2023). HD 191939 revisited: New and refined planet mass determinations, and a new planet in the habitable zone. *Astronomy and Astrophysics*, 669:A40. ADS Bibcode: 2023A&A...669A..40O.

Palle, E., Nowak, G., Luque, R., Hidalgo, D., Barragán, O., Prieto-Arranz, J., Hirano, T., Fridlund, M., Gandolfi, D., Livingston, J., Dai, F., Morales, J. C., Lafarga, M., Albrecht, S., Alonso, R., Amado, P. J., Caballero, J. A., Cabrera, J., Cochran, W. D., Csizmadia, S., Deeg, H., Eigmüller, P., Endl, M., Erikson, A., Fukui, A., Guenther, E. W., Grziwa, S., Hatzes, A. P., Korth, J., Kürster, M., Kuzuhara, M., Montañes Rodríguez, P., Murgas, F., Narita, N., Nespral, D., Pätzold, M., Persson, C. M., Quirrenbach, A., Rauer, H., Redfield, S., Reiners, A., Ribas, I., Smith, A. M. S., Van Eylen, V., Winn, J. N., and Zechmeister, M. (2019). Detection and Doppler monitoring of K2-285 (EPIC 246471491), a system of four transiting planets smaller than Neptune. *Astronomy and Astrophysics*, 623:A41. ADS Bibcode: 2019A&A...623A..41P.

Quintana, E. V., Barclay, T., Raymond, S. N., Rowe, J. F., Bolmont, E., Caldwell, D. A., Howell, S. B., Kane, S. R., Huber, D., Crepp, J. R., Lissauer, J. J., Ciardi, D. R., Coughlin, J. L., Everett, M. E., Henze, C. E., Horch, E., Isaacson, H., Ford, E. B., Adams, F. C., Still, M., Hunter, R. C., Quarles, B., and Selsis, F. (2014). An Earth-Sized Planet in the Habitable Zone of a Cool Star. *Science*, 344:277–280. ADS Bibcode: 2014Sci...344..277Q.

Rein, H. and Liu, S.-F. (2012). REBOUND: an open-source multi-purpose N -body code for collisional dynamics. *Astronomy & Astrophysics*, 537:A128.

Rodriguez, J. E., Becker, J. C., Eastman, J. D., Hadden, S., Vanderburg, A., Khain, T., Quinn, S. N., Mayo, A., Dressing, C. D., Schlieder, J. E., Ciardi, D. R., Latham, D. W., Rappaport, S., Adams, F. C., Berlind, P., Bieryla, A., Calkins, M. L., Esquerdo, G. A., Kristiansen, M. H., Omohundro, M., Schwengeler, H. M., Stassun, K. G., and Terentev, I. (2018). A Compact Multi-planet System with a Significantly Misaligned Ultra Short Period Planet. *The Astronomical Journal*, 156:245. Publisher: IOP ADS Bibcode: 2018AJ....156..245R.

Rowe, J. F., Bryson, S. T., Marcy, G. W., Lissauer, J. J., Jontof-Hutter, D., Mullally, F., Gilliland, R. L., Issacson, H., Ford, E., Howell, S. B., Borucki, W. J., Haas, M., Huber, D., Steffen, J. H., Thompson, S. E., Quintana, E., Barclay, T., Still, M., Fortney, J., Gautier, III, T. N., Hunter, R., Caldwell, D. A., Ciardi, D. R., Devore, E., Cochran, W., Jenkins, J., Agol, E., Carter, J. A., and Geary, J. (2014). Validation of Kepler's Multiple Planet Candidates. III. Light Curve Analysis and Announcement of Hundreds of New Multi-planet Systems. *The Astrophysical Journal*, 784:45. Publisher: IOP ADS Bibcode: 2014ApJ...784...45R.

Schmitt, J. R., Jenkins, J. M., and Fischer, D. A. (2017). A Search for Lost Planets in the

Kepler Multi-planet Systems and the Discovery of the Long-period, Neptune-sized Exoplanet Kepler-150 f. *The Astronomical Journal*, 153:180. Publisher: IOP ADS Bibcode: 2017AJ....153..180S.

Torres, G., Kipping, D. M., Fressin, F., Caldwell, D. A., Twicken, J. D., Ballard, S., Batalha, N. M., Bryson, S. T., Ciardi, D. R., Henze, C. E., Howell, S. B., Isaacson, H. T., Jenkins, J. M., Muirhead, P. S., Newton, E. R., Petigura, E. A., Barclay, T., Borucki, W. J., Crepp, J. R., Everett, M. E., Horch, E. P., Howard, A. W., Kolbl, R., Marcy, G. W., McCauliff, S., and Quintana, E. V. (2015). Validation of 12 Small Kepler Transiting Planets in the Habitable Zone. *The Astrophysical Journal*, 800:99. Publisher: IOP ADS Bibcode: 2015ApJ...800...99T.

Turtelboom, E. V., Weiss, L. M., Dressing, C. D., Nowak, G., Pallé, E., Beard, C., Blunt, S., Brinkman, C., Chontos, A., Claytor, Z. R., Dai, F., Dalba, P. A., Giacalone, S., Gonzales, E., Harada, C. K., Hill, M. L., Holcomb, R., Korth, J., Lubin, J., Masseron, T., MacDougall, M., Mayo, A. W., Močnik, T., Akana Murphy, J. M., Polanski, A. S., Rice, M., Rubenzahl, R. A., Scarsdale, N., Stassun, K. G., Tyler, D. B., Zandt, J. V., Crossfield, I. J. M., Deeg, H. J., Fulton, B., Gandolfi, D., Howard, A. W., Huber, D., Isaacson, H., Kane, S. R., Lam, K. W. F., Luque, R., Martín, E. L., Morello, G., Orell-Miquel, J., Petigura, E. A., Robertson, P., Roy, A., Van Eylen, V., Baker, D., Belinski, A. A., Bieryla, A., Ciardi, D. R., Collins, K. A., Cutting, N., Della-Rose, D. J., Ellingsen, T. B., Furlan, E., Gan, T., Gnilka, C. L., Guerra, P., Howell, S. B., Jimenez, M., Latham, D. W., Larivière, M., Lester, K. V., Lillo-Box, J., Luker, L., Mann, C. R., Plavchan, P. P., Safonov, B., Skinner, B., Strakhov, I. A., Wittrock, J. M., Caldwell, D. A., Essack, Z., Jenkins, J. M., Quintana, E. V., Ricker, G. R., Vanderspek, R., Seager, S., and Winn, J. N. (2022). The TESS-Keck Survey. XI. Mass Measurements for Four Transiting Sub-Neptunes Orbiting K Dwarf TOI-1246. *The Astronomical Journal*, 163:293. Publisher: IOP ADS Bibcode: 2022AJ....163..293T.

Virtanen, P., Gommers, R., Oliphant, T. E., Haberland, M., Reddy, T., Cournapeau, D., Burovski, E., Peterson, P., Weckesser, W., Bright, J., van der Walt, S. J., Brett, M., Wilson, J., Millman, K. J., Mayorov, N., Nelson, A. R. J., Jones, E., Kern, R., Larson, E., Carey, C. J., Polat, , Feng, Y., Moore, E. W., VanderPlas, J., Laxalde, D., Perktold, J., Cimrman, R., Henriksen, I., Quintero, E. A., Harris, C. R., Archibald, A. M., Ribeiro, A. H., Pedregosa, F., van Mulbregt, P., SciPy 1.0 Contributors, Vijaykumar, A., Bardelli, A. P., Rothberg, A., Hilboll, A., Kloekner, A., Scopatz, A., Lee, A., Rokem, A., Woods, C. N., Fulton, C., Masson, C., Häggström, C., Fitzgerald, C., Nicholson, D. A., Hagen, D. R., Pasechnik, D. V., Olivetti, E., Martin, E., Wieser, E., Silva, F.,

Lenders, F., Wilhelm, F., Young, G., Price, G. A., Ingold, G.-L., Allen, G. E., Lee, G. R., Audren, H., Probst, I., Dietrich, J. P., Silterra, J., Webber, J. T., Slavič, J., Nothman, J., Buchner, J., Kulick, J., Schönberger, J. L., de Miranda Cardoso, J. V., Reimer, J., Harrington, J., Rodríguez, J. L. C., Nunez-Iglesias, J., Kuczynski, J., Tritz, K., Thoma, M., Newville, M., Kümmeler, M., Bolingbroke, M., Tartre, M., Pak, M., Smith, N. J., Nowaczyk, N., Shebanov, N., Pavlyk, O., Brodtkorb, P. A., Lee, P., McGibbon, R. T., Feldbauer, R., Lewis, S., Tygier, S., Sievert, S., Vigna, S., Peterson, S., More, S., Pudlik, T., Oshima, T., Pingel, T. J., Robitaille, T. P., Spura, T., Jones, T. R., Cera, T., Leslie, T., Zito, T., Krauss, T., Upadhyay, U., Halchenko, Y. O., and Vázquez-Baeza, Y. (2020). SciPy 1.0: fundamental algorithms for scientific computing in Python. *Nature Methods*, 17(3):261–272.

Weiss, L. M., Marcy, G. W., Rowe, J. F., Howard, A. W., Isaacson, H., Fortney, J. J., Miller, N., Demory, B.-O., Fischer, D. A., Adams, E. R., Dupree, A. K., Howell, S. B., Kolbl, R., Johnson, J. A., Horch, E. P., Everett, M. E., Fabrycky, D. C., and Seager, S. (2013). The Mass of KOI-94d and a Relation for Planet Radius, Mass, and Incident Flux. *The Astrophysical Journal*, 768:14. Publisher: IOP ADS Bibcode: 2013ApJ...768...14W.

Wells, R., Poppenhaeger, K., and Watson, C. A. (2019). Validation of a temperate fourth planet in the K2-133 multiplanet system. *Monthly Notices of the Royal Astronomical Society*, 487:1865–1873. Publisher: OUP ADS Bibcode: 2019MNRAS.487.1865W.

A System by System Priors

Table 4: Priors for the stellar mass used for each system and the relevant citation for stellar parameters. Items marked with a star did not have complete constraints on the variable (most likely value and $\pm 1\sigma$ bounds) and were thus populated with an uninformed prior subject to the available data (see text). Empirical denotes that there was no stellar mass data published and the mass was instead drawn from the empirical distribution presented in Figure 2.

| System | Stellar Mass Prior (M_{\odot}) | Citation |
|------------|------------------------------------|-------------------------|
| HD 108236 | $U(0.820, 0.920)$ | Bonfanti et al. (2021) |
| HD 191939 | $U(0.770, 0.850)$ | Lubin et al. (2022) |
| HD 23472 | $U(0.640, 0.700)$ | Barros et al. (2022) |
| K2-133 | $U(0.450, 0.470)$ | Wells et al. (2019) |
| K2-138 | $U(0.920, 0.960)$ | Lopez et al. (2019) |
| K2-266 | $U(0.660, 0.720)$ | Rodriguez et al. (2018) |
| K2-285 | $U(0.810, 0.850)$ | Palle et al. (2019) |
| K2-32 | $U(0.810, 0.850)$ | Lillo-Box et al. (2020) |
| K2-72 | $U(0.180, 0.350)$ | Dressing et al. (2017) |
| KOI-94 | $U(1.230, 1.330)$ | Weiss et al. (2013) |
| Kepler-102 | $U(0.780, 0.820)$ | Bonomo et al. (2023) |
| Kepler-107 | $U(1.210, 1.270)$ | Bonomo et al. (2023) |
| Kepler-11 | $U(0.930, 0.990)$ | Lissauer et al. (2013) |
| Kepler-150 | Emperical* | Rowe et al. (2014) |
| Kepler-167 | $U(0.750, 0.810)$ | Chachan et al. (2022) |
| Kepler-169 | Emperical* | Rowe et al. (2014) |
| Kepler-172 | Emperical* | Rowe et al. (2014) |
| Kepler-186 | $U(0.420, 0.540)$ | Quintana et al. (2014) |
| Kepler-197 | Emperical* | Rowe et al. (2014) |
| Kepler-20 | $U(0.880, 0.980)$ | Bonomo et al. (2023) |
| Kepler-208 | Emperical* | Rowe et al. (2014) |
| Kepler-215 | Emperical* | Rowe et al. (2014) |
| Kepler-220 | Emperical* | Rowe et al. (2014) |
| Kepler-221 | Emperical* | Rowe et al. (2014) |
| Kepler-224 | Emperical* | Rowe et al. (2014) |
| Kepler-235 | Emperical* | Rowe et al. (2014) |
| Kepler-24 | $U(0.890, 1.140)$ | Ford et al. (2012) |
| Kepler-251 | Emperical* | Rowe et al. (2014) |

| | | |
|------------|-------------------|-----------------------------|
| Kepler-256 | Emperical* | Rowe et al. (2014) |
| Kepler-265 | Emperical* | Rowe et al. (2014) |
| Kepler-286 | Emperical* | Rowe et al. (2014) |
| Kepler-292 | Emperical* | Rowe et al. (2014) |
| Kepler-296 | $U(0.410, 0.570)$ | Barclay et al. (2015) |
| Kepler-299 | Emperical* | Rowe et al. (2014) |
| Kepler-306 | Emperical* | Rowe et al. (2014) |
| Kepler-32 | $U(0.530, 0.630)$ | Fabrycky et al. (2012) |
| Kepler-33 | $U(1.170, 1.350)$ | Lissauer et al. (2012) |
| Kepler-341 | Emperical* | Rowe et al. (2014) |
| Kepler-402 | Emperical* | Rowe et al. (2014) |
| Kepler-444 | $U(0.720, 0.800)$ | Campante et al. (2015) |
| Kepler-62 | $U(0.670, 0.710)$ | Borucki et al. (2013) |
| Kepler-79 | $U(1.130, 1.210)$ | Jontof-Hutter et al. (2014) |
| Kepler-82 | $U(0.880, 0.940)$ | Freudenthal et al. (2019) |
| TOI-1246 | $U(0.840, 0.900)$ | Turtelboom et al. (2022) |
| TOI-178 | $U(0.620, 0.680)$ | Leleu et al. (2021) |
| TOI-561 | $U(0.770, 0.850)$ | Lacedelli et al. (2022) |
| TOI-700 | $U(0.390, 0.430)$ | Gilbert et al. (2023) |
| TRAPPIST-1 | Emperical* | Agol et al. (2021) |
| V1298 Tau | $U(1.050, 1.150)$ | David et al. (2019) |

Table 5: Priors for the planetary mass, semi-major axis, eccentricity, and, if relevant, the planetary radius used for each planet along with the relevant citation for planetary parameters parameters. Items marked with a star did not have complete constraints on the variable (most likely value and $\pm 1\sigma$ bounds) and were thus populated with an uninformed prior subject to the available data (see text). Mass-Radius denotes that there was no planetary mass data published, or only an upper bound was published, and the mass was instead drawn using mass-radius relations using `forecaster` (Chen and Kipping, 2017).

| Planet Name | Mass Prior (M_{\oplus}) | Semi-Major Axis Prior (au) | Eccentricity Prior | Radius Prior (R_{\oplus}) | Citation |
|-------------|-----------------------------|----------------------------|--------------------|-------------------------------|----------------------------|
| HD 108236 b | Mass-Radius* | $U(0.0444, 0.0462)$ | $U(0.012, 0.084)$ | $U(1.564, 1.666)$ | Bonfanti et al. (2021) |
| HD 108236 c | Mass-Radius* | $U(0.0608, 0.0632)$ | $U(0.009, 0.076)$ | $U(2.019, 2.123)$ | Bonfanti et al. (2021) |
| HD 108236 d | Mass-Radius* | $U(0.1051, 0.1097)$ | $U(0.02, 0.093)$ | $U(2.474, 2.601)$ | Bonfanti et al. (2021) |
| HD 108236 e | Mass-Radius* | $U(0.1347, 0.1389)$ | $U(0.022, 0.09)$ | $U(3.031, 3.135)$ | Bonfanti et al. (2021) |
| HD 108236 f | Mass-Radius* | $U(0.1720, 0.1799)$ | $U(0.017, 0.087)$ | $U(1.96, 2.069)$ | Bonfanti et al. (2021) |
| HD 191939 b | $U(9.3, 10.7)$ | $U(0.0781, 0.0829)$ | $U(0.02, 0.041)$ | N/A | Orell-Miquel et al. (2023) |
| HD 191939 c | $U(7, 9)$ | $U(0.1702, 0.1807)$ | $U(0.021, 0.068)$ | N/A | Orell-Miquel et al. (2023) |
| HD 191939 d | $U(2.2, 3.4)$ | $U(0.2071, 0.2197)$ | $U(0.019, 0.049)$ | N/A | Orell-Miquel et al. (2023) |
| HD 191939 g | Mass-Radius* | $U(0.7840, 0.8400)$ | $U(0.019, 0.055)$ | $U(nan, nan)^*$ | Orell-Miquel et al. (2023) |
| HD 23472 b | $U(0.35, 0.76)$ | $U(0.0423, 0.0436)$ | $U(0.023, 0.12)$ | N/A | Barros et al. (2022) |
| HD 23472 c | $U(0.45, 1)$ | $U(0.0670, 0.0690)$ | $U(0.023, 0.122)$ | N/A | Barros et al. (2022) |
| HD 23472 d | $U(0.37, 1.21)$ | $U(0.0892, 0.0920)$ | $U(0.019, 0.118)$ | N/A | Barros et al. (2022) |
| HD 23472 e | $U(7.53, 9.1)$ | $U(0.1144, 0.1180)$ | $U(0.032, 0.111)$ | N/A | Barros et al. (2022) |
| HD 23472 f | $U(2.6, 4.29)$ | $U(0.1622, 0.1670)$ | $U(0.02, 0.117)$ | N/A | Barros et al. (2022) |
| K2-133 b | Mass-Radius* | $U(0.0317, 0.0322)$ | 0* | $U(1.264, 1.417)$ | Wells et al. (2019) |
| K2-133 c | Mass-Radius* | $U(0.0431, 0.0437)$ | 0* | $U(1.515, 1.693)$ | Wells et al. (2019) |
| K2-133 d | Mass-Radius* | $U(0.0743, 0.0755)$ | 0* | $U(1.896, 2.11)$ | Wells et al. (2019) |
| K2-133 e | Mass-Radius* | $U(0.1335, 0.1357)$ | 0* | $U(1.6, 1.87)$ | Wells et al. (2019) |
| K2-138 b | $U(2.05, 4.15)$ | $U(0.0336, 0.0341)$ | $U(0.015, 0.102)$ | N/A | Lopez et al. (2019) |
| K2-138 c | $U(5.08, 7.44)$ | $U(0.0442, 0.0449)$ | $U(0.013, 0.096)$ | N/A | Lopez et al. (2019) |
| K2-138 d | $U(6.57, 9.31)$ | $U(0.0584, 0.0593)$ | $U(0.013, 0.084)$ | N/A | Lopez et al. (2019) |
| K2-138 e | $U(10.98, 14.95)$ | $U(0.0775, 0.0787)$ | $U(0.028, 0.125)$ | N/A | Lopez et al. (2019) |
| K2-138 f | $U(0.45, 3.75)$ | $U(0.1036, 0.1052)$ | $U(0.019, 0.126)$ | N/A | Lopez et al. (2019) |
| K2-138 g | $U(1.29, 9.58)$ | $U(0.2291, 0.2326)$ | $U(0.019, 0.122)$ | N/A | Lopez et al. (2019) |
| K2-266 b | Mass-Radius* | $U(0.0129, 0.0133)$ | 0* | $U(2, 5.1)$ | Rodriguez et al. (2018) |

| | | | | | |
|--------------|-----------------------------|---------------------|----------------------|-------------------|-------------------------|
| K2-266 c | Mass-Radius* | $U(0.0668, 0.0690)$ | $U(0.012, 0.085)$ | $U(0.62, 0.801)$ | Rodriguez et al. (2018) |
| K2-266 d | $U(5.1, 14.6)$ | $U(0.1018, 0.1051)$ | $U(0.015, 0.09)$ | N/A | Rodriguez et al. (2018) |
| K2-266 e | $U(9.3, 20.7)$ | $U(0.1229, 0.1268)$ | $U(0.013, 0.079)$ | N/A | Rodriguez et al. (2018) |
| K2-285 b | $U(8.31, 10.89)$ | $U(0.0373, 0.0391)$ | 0* | N/A | Palle et al. (2019) |
| K2-285 c | $U(13.55, 17.96)$ | $U(0.0806, 0.0842)$ | 0* | N/A | Palle et al. (2019) |
| K2-285 d | Mass-Radius ($M < 6.5$)* | $U(0.1149, 0.1207)$ | 0* | $U(2.42, 2.54)$ | Palle et al. (2019) |
| K2-285 e | Mass-Radius ($M < 10.7$)* | $U(0.1761, 0.1846)$ | 0* | $U(1.9, 2)$ | Palle et al. (2019) |
| K2-32 b | $U(1, 3.4)$ | $U(0.0486, 0.0494)$ | $U(0.013, 0.091)$ | N/A | Lillo-Box et al. (2020) |
| K2-32 c | $U(13.3, 16.8)$ | $U(0.0789, 0.0802)$ | $U(0.009, 0.062)$ | N/A | Lillo-Box et al. (2020) |
| K2-32 d | $U(5.7, 10.5)$ | $U(0.1373, 0.1396)$ | $U(0.014, 0.095)$ | N/A | Lillo-Box et al. (2020) |
| K2-32 e | $U(4.2, 9.2)$ | $U(0.1828, 0.1857)$ | $U(0.015, 0.103)$ | N/A | Lillo-Box et al. (2020) |
| K2-72 b | Mass-Radius* | $U(0.0350, 0.0440)$ | $U(0.02234, 0.307)$ | $U(0.97, 1.19)$ | Dressing et al. (2017) |
| K2-72 c | Mass-Radius* | $U(0.0440, 0.0540)$ | $U(0.01767, 0.3178)$ | $U(0.89, 1.13)$ | Dressing et al. (2017) |
| K2-72 d | Mass-Radius* | $U(0.0680, 0.0850)$ | $U(0.01846, 0.312)$ | $U(1.03, 1.29)$ | Dressing et al. (2017) |
| K2-72 e | Mass-Radius* | $U(0.0930, 0.1150)$ | $U(0.02317, 0.3087)$ | $U(1.16, 1.43)$ | Dressing et al. (2017) |
| KOI-94 b | $U(5.9, 15.1)$ | $U(0.0505, 0.0519)$ | $U(0.08, 0.42)$ | N/A | Weiss et al. (2013) |
| KOI-94 c | $U(0, 21.3)$ | $U(0.1000, 0.1026)$ | $U(0.2, 0.66)$ | N/A | Weiss et al. (2013) |
| KOI-94 d | $U(95, 117)$ | $U(0.1662, 0.1706)$ | $U(0, 0.06)$ | N/A | Weiss et al. (2013) |
| KOI-94 e | $U(7, 53)$ | $U(0.3006, 0.3086)$ | $U(0, 0.249)$ | N/A | Weiss et al. (2013) |
| Kepler-102 b | Mass-Radius ($M < 1.1$)* | $U(0.0547, 0.0557)$ | 0* | $U(0.434, 0.486)$ | Bonomo et al. (2023) |
| Kepler-102 c | Mass-Radius ($M < 1.7$)* | $U(0.0664, 0.0676)$ | 0* | $U(0.539, 0.595)$ | Bonomo et al. (2023) |
| Kepler-102 d | $U(1.7, 4.3)$ | $U(0.0854, 0.0869)$ | 0* | N/A | Bonomo et al. (2023) |
| Kepler-102 e | $U(2.9, 6.5)$ | $U(0.1152, 0.1172)$ | 0* | N/A | Bonomo et al. (2023) |
| Kepler-102 f | Mass-Radius ($M < 4.3$)* | $U(0.1641, 0.1671)$ | 0* | $U(0.839, 0.883)$ | Bonomo et al. (2023) |
| Kepler-107 b | $U(2.1, 5.6)$ | $U(0.0451, 0.0458)$ | 0* | N/A | Bonomo et al. (2023) |
| Kepler-107 c | $U(8, 12)$ | $U(0.0602, 0.0611)$ | 0* | N/A | Bonomo et al. (2023) |
| Kepler-107 d | Mass-Radius ($M < 7.7$)* | $U(0.0831, 0.0844)$ | 0* | $U(0.8, 0.92)$ | Bonomo et al. (2023) |
| Kepler-107 e | $U(10.8, 17.4)$ | $U(0.1254, 0.1274)$ | 0* | N/A | Bonomo et al. (2023) |
| Kepler-11 b | $U(0.9, 3.3)$ | $U(0.0900, 0.0920)$ | $U(0.003, 0.113)$ | N/A | Lissauer et al. (2013) |
| Kepler-11 c | $U(1.3, 5.8)$ | $U(0.1060, 0.1080)$ | $U(0.013, 0.089)$ | N/A | Lissauer et al. (2013) |
| Kepler-11 d | $U(5.8, 8.1)$ | $U(0.1540, 0.1560)$ | $U(0.002, 0.011)$ | N/A | Lissauer et al. (2013) |

| | | | | | |
|--------------|---------------------------|----------------------|-------------------|-------------------|------------------------|
| Kepler-11 e | $U(5.9, 9.5)$ | $U(0.1930, 0.1970)$ | $U(0.006, 0.018)$ | N/A | Lissauer et al. (2013) |
| Kepler-11 f | $U(1.1, 2.8)$ | $U(0.2480, 0.2520)$ | $U(0.004, 0.024)$ | N/A | Lissauer et al. (2013) |
| Kepler-11 g | Mass-Radius ($M < 25$)* | $U(0.4620, 0.4700)$ | 0* | $U(3.25, 3.39)$ | Lissauer et al. (2013) |
| Kepler-150 b | Mass-Radius* | $U(0.0352, 0.0528)*$ | 0* | $U(1.06, 1.44)$ | Rowe et al. (2014) |
| Kepler-150 c | Mass-Radius* | $U(0.0584, 0.0876)*$ | 0* | $U(3.1, 4.28)$ | Rowe et al. (2014) |
| Kepler-150 d | Mass-Radius* | $U(0.0832, 0.1248)*$ | 0* | $U(2.38, 3.2)$ | Rowe et al. (2014) |
| Kepler-150 e | Mass-Radius* | $U(0.1512, 0.2268)*$ | 0* | $U(2.57, 3.67)$ | Rowe et al. (2014) |
| Kepler-150 f | Mass-Radius* | $U(0.7900, 1.5300)$ | 0* | $U(3.25, 4.16)$ | Schmitt et al. (2017) |
| Kepler-167 b | Mass-Radius* | $U(0.0476, 0.0490)$ | 0* | $U(1.648, 1.788)$ | Chachan et al. (2022) |
| Kepler-167 c | Mass-Radius* | $U(0.0674, 0.0694)$ | 0* | $U(1.605, 1.743)$ | Chachan et al. (2022) |
| Kepler-167 d | Mass-Radius* | $U(0.1384, 0.1424)$ | 0* | $U(1.174, 1.302)$ | Chachan et al. (2022) |
| Kepler-167 e | $U(273.3, 371.9)$ | $U(1.8560, 1.9100)$ | 0* | N/A | Chachan et al. (2022) |
| Kepler-169 b | Mass-Radius* | $U(0.032, 0.048)*$ | 0* | $U(1.05, 1.21)$ | Rowe et al. (2014) |
| Kepler-169 c | Mass-Radius* | $U(0.0496, 0.0744)*$ | 0* | $U(1.13, 1.29)$ | Rowe et al. (2014) |
| Kepler-169 d | Mass-Radius* | $U(0.06, 0.09)*$ | 0* | $U(1.16, 1.34)$ | Rowe et al. (2014) |
| Kepler-169 e | Mass-Radius* | $U(0.084, 0.126)*$ | 0* | $U(1.91, 2.49)$ | Rowe et al. (2014) |
| Kepler-169 f | Mass-Radius* | $U(0.2872, 0.4308)*$ | 0* | $U(2.34, 2.82)$ | Rowe et al. (2014) |
| Kepler-172 b | Mass-Radius* | $U(0.032, 0.048)*$ | 0* | $U(1.93, 2.77)$ | Rowe et al. (2014) |
| Kepler-172 c | Mass-Radius* | $U(0.0544, 0.0816)*$ | 0* | $U(2.33, 3.39)$ | Rowe et al. (2014) |
| Kepler-172 d | Mass-Radius* | $U(0.0944, 0.1416)*$ | 0* | $U(1.85, 2.65)$ | Rowe et al. (2014) |
| Kepler-172 e | Mass-Radius* | $U(0.1688, 0.2532)*$ | 0* | $U(2.2, 3.32)$ | Rowe et al. (2014) |
| Kepler-186 b | Mass-Radius* | $U(0.0297, 0.0389)$ | 0* | $U(0.95, 1.19)$ | Quintana et al. (2014) |
| Kepler-186 c | Mass-Radius* | $U(0.0381, 0.0521)$ | 0* | $U(1.11, 1.39)$ | Quintana et al. (2014) |
| Kepler-186 d | Mass-Radius* | $U(0.0681, 0.0881)$ | 0* | $U(1.24, 1.56)$ | Quintana et al. (2014) |
| Kepler-186 e | Mass-Radius* | $U(0.0950, 0.1250)$ | 0* | $U(1.13, 1.42)$ | Quintana et al. (2014) |
| Kepler-186 f | Mass-Radius* | $U(0.3790, 0.6030)$ | $U(0, 0.11)$ | $U(1.09, 1.25)$ | Torres et al. (2015) |
| Kepler-197 b | Mass-Radius* | $U(0.048, 0.072)*$ | 0* | $U(0.98, 1.06)$ | Rowe et al. (2014) |
| Kepler-197 c | Mass-Radius* | $U(0.072, 0.108)*$ | 0* | $U(1.19, 1.27)$ | Rowe et al. (2014) |
| Kepler-197 d | Mass-Radius* | $U(0.0952, 0.1428)*$ | 0* | $U(1.12, 1.32)$ | Rowe et al. (2014) |
| Kepler-197 e | Mass-Radius* | $U(0.1312, 0.1968)*$ | 0* | $U(0.87, 0.95)$ | Rowe et al. (2014) |
| Kepler-20 b | $U(8.4, 11)$ | $U(0.0448, 0.0465)$ | 0* | N/A | Bonomo et al. (2023) |

| | | | | | |
|--------------|------------------------------|-----------------------|----|-------------------|----------------------|
| Kepler-20 c | Mass-Radius ($M < 0.76$)* | $U(0.0625, 0.0649)$ | 0* | $U(0.799, 0.843)$ | Bonomo et al. (2023) |
| Kepler-20 d | $U(9, 13.2)$ | $U(0.0918, 0.0954)$ | 0* | N/A | Bonomo et al. (2023) |
| Kepler-20 e | Mass-Radius ($M < 1.4$)* | $U(0.1360, 0.1414)$ | 0* | $U(0.865, 0.999)$ | Bonomo et al. (2023) |
| Kepler-20 f | $U(9.8, 17.1)$ | $U(0.3407, 0.3541)$ | 0* | N/A | Bonomo et al. (2023) |
| Kepler-208 b | Mass-Radius* | $U(0.0432, 0.0648)^*$ | 0* | $U(1.33, 1.93)$ | Rowe et al. (2014) |
| Kepler-208 c | Mass-Radius* | $U(0.0632, 0.0948)^*$ | 0* | $U(1.13, 1.65)$ | Rowe et al. (2014) |
| Kepler-208 d | Mass-Radius* | $U(0.0824, 0.1236)^*$ | 0* | $U(0.97, 1.43)$ | Rowe et al. (2014) |
| Kepler-208 e | Mass-Radius* | $U(0.1056, 0.1584)^*$ | 0* | $U(1.2, 1.76)$ | Rowe et al. (2014) |
| Kepler-215 b | Mass-Radius* | $U(0.0672, 0.1008)^*$ | 0* | $U(1.22, 2.02)$ | Rowe et al. (2014) |
| Kepler-215 c | Mass-Radius* | $U(0.0904, 0.1356)^*$ | 0* | $U(1.35, 2.19)$ | Rowe et al. (2014) |
| Kepler-215 d | Mass-Radius* | $U(0.148, 0.222)^*$ | 0* | $U(1.84, 2.94)$ | Rowe et al. (2014) |
| Kepler-215 e | Mass-Radius* | $U(0.2512, 0.3768)^*$ | 0* | $U(1.34, 2.16)$ | Rowe et al. (2014) |
| Kepler-220 b | Mass-Radius* | $U(0.0368, 0.0552)^*$ | 0* | $U(0.76, 0.86)$ | Rowe et al. (2014) |
| Kepler-220 c | Mass-Radius* | $U(0.0608, 0.0912)^*$ | 0* | $U(1.48, 1.66)$ | Rowe et al. (2014) |
| Kepler-220 d | Mass-Radius* | $U(0.1304, 0.1956)^*$ | 0* | $U(0.92, 1.04)$ | Rowe et al. (2014) |
| Kepler-220 e | Mass-Radius* | $U(0.1808, 0.2712)^*$ | 0* | $U(1.21, 1.45)$ | Rowe et al. (2014) |
| Kepler-221 b | Mass-Radius* | $U(0.0296, 0.0444)^*$ | 0* | $U(1.54, 1.88)$ | Rowe et al. (2014) |
| Kepler-221 c | Mass-Radius* | $U(0.0472, 0.0708)^*$ | 0* | $U(2.66, 3.2)$ | Rowe et al. (2014) |
| Kepler-221 d | Mass-Radius* | $U(0.0696, 0.1044)^*$ | 0* | $U(2.48, 2.98)$ | Rowe et al. (2014) |
| Kepler-221 e | Mass-Radius* | $U(0.104, 0.156)^*$ | 0* | $U(2.38, 2.88)$ | Rowe et al. (2014) |
| Kepler-224 b | Mass-Radius* | $U(0.0304, 0.0456)^*$ | 0* | $U(1.3, 1.48)$ | Rowe et al. (2014) |
| Kepler-224 c | Mass-Radius* | $U(0.0464, 0.0696)^*$ | 0* | $U(2.86, 3.38)$ | Rowe et al. (2014) |
| Kepler-224 d | Mass-Radius* | $U(0.0712, 0.1068)^*$ | 0* | $U(2.16, 2.44)$ | Rowe et al. (2014) |
| Kepler-224 e | Mass-Radius* | $U(0.0992, 0.1488)^*$ | 0* | $U(1.82, 2.12)$ | Rowe et al. (2014) |
| Kepler-235 b | Mass-Radius* | $U(0.0296, 0.0444)^*$ | 0* | $U(2.13, 2.33)$ | Rowe et al. (2014) |
| Kepler-235 c | Mass-Radius* | $U(0.052, 0.078)^*$ | 0* | $U(1.2, 1.36)$ | Rowe et al. (2014) |
| Kepler-235 d | Mass-Radius* | $U(0.0976, 0.1464)^*$ | 0* | $U(1.95, 2.15)$ | Rowe et al. (2014) |
| Kepler-235 e | Mass-Radius* | $U(0.1704, 0.2556)^*$ | 0* | $U(1.93, 2.51)$ | Rowe et al. (2014) |
| Kepler-24 b | Mass-Radius* | $U(0.0408, 0.0612)^*$ | 0* | $U(1.28, 2.06)$ | Ford et al. (2012) |
| Kepler-24 c | Mass-Radius ($M < 508.5$)* | $U(0.064, 0.096)^*$ | 0* | $U(1.92, 2.88)^*$ | Ford et al. (2012) |
| Kepler-24 d | Mass-Radius ($M < 508.5$)* | $U(0.0848, 0.1272)^*$ | 0* | $U(2.24, 3.36)^*$ | Rowe et al. (2014) |

| | | | | | | |
|--|--------------|--------------|-----------------------|----|-----------------|-----------------------|
| | Kepler-24 e | Mass-Radius* | $U(0.1104, 0.1656)^*$ | 0* | $U(2.14, 3.42)$ | Rowe et al. (2014) |
| | Kepler-251 b | Mass-Radius* | $U(0.0424, 0.0636)^*$ | 0* | $U(1.09, 1.57)$ | Rowe et al. (2014) |
| | Kepler-251 c | Mass-Radius* | $U(0.0976, 0.1464)^*$ | 0* | $U(2.28, 3.26)$ | Rowe et al. (2014) |
| | Kepler-251 d | Mass-Radius* | $U(0.1456, 0.2184)^*$ | 0* | $U(2.28, 3.26)$ | Rowe et al. (2014) |
| | Kepler-251 e | Mass-Radius* | $U(0.3232, 0.4848)^*$ | 0* | $U(2.28, 3.26)$ | Rowe et al. (2014) |
| | Kepler-256 b | Mass-Radius* | $U(0.0216, 0.0324)^*$ | 0* | $U(1.2, 1.98)$ | Rowe et al. (2014) |
| | Kepler-256 c | Mass-Radius* | $U(0.036, 0.054)^*$ | 0* | $U(1.62, 2.68)$ | Rowe et al. (2014) |
| | Kepler-256 d | Mass-Radius* | $U(0.0512, 0.0768)^*$ | 0* | $U(1.85, 3.11)$ | Rowe et al. (2014) |
| | Kepler-256 e | Mass-Radius* | $U(0.0768, 0.1152)^*$ | 0* | $U(1.77, 2.93)$ | Rowe et al. (2014) |
| | Kepler-265 b | Mass-Radius* | $U(0.0552, 0.0828)^*$ | 0* | $U(1.41, 2.31)$ | Rowe et al. (2014) |
| | Kepler-265 c | Mass-Radius* | $U(0.1016, 0.1524)^*$ | 0* | $U(2.08, 3.18)$ | Rowe et al. (2014) |
| | Kepler-265 d | Mass-Radius* | $U(0.1888, 0.2832)^*$ | 0* | $U(1.95, 3.03)$ | Rowe et al. (2014) |
| | Kepler-265 e | Mass-Radius* | $U(0.2552, 0.3828)^*$ | 0* | $U(2.04, 3.14)$ | Rowe et al. (2014) |
| | Kepler-286 b | Mass-Radius* | $U(0.0216, 0.0324)^*$ | 0* | $U(0.99, 1.49)$ | Rowe et al. (2014) |
| | Kepler-286 c | Mass-Radius* | $U(0.0336, 0.0504)^*$ | 0* | $U(1.1, 1.64)$ | Rowe et al. (2014) |
| | Kepler-286 d | Mass-Radius* | $U(0.0488, 0.0732)^*$ | 0* | $U(1.06, 1.6)$ | Rowe et al. (2014) |
| | Kepler-286 e | Mass-Radius* | $U(0.1408, 0.2112)^*$ | 0* | $U(1.34, 2.2)$ | Rowe et al. (2014) |
| | Kepler-292 b | Mass-Radius* | $U(0.028, 0.042)^*$ | 0* | $U(1.18, 1.46)$ | Rowe et al. (2014) |
| | Kepler-292 c | Mass-Radius* | $U(0.036, 0.054)^*$ | 0* | $U(1.32, 1.62)$ | Rowe et al. (2014) |
| | Kepler-292 d | Mass-Radius* | $U(0.0544, 0.0816)^*$ | 0* | $U(2.02, 2.44)$ | Rowe et al. (2014) |
| | Kepler-292 e | Mass-Radius* | $U(0.0776, 0.1164)^*$ | 0* | $U(2.32, 3.02)$ | Rowe et al. (2014) |
| | Kepler-292 f | Mass-Radius* | $U(0.1128, 0.1692)^*$ | 0* | $U(2.13, 2.57)$ | Rowe et al. (2014) |
| | Kepler-296 b | Mass-Radius* | $U(0.0435, 0.0609)$ | 0* | $U(1.68, 2.33)$ | Barclay et al. (2015) |
| | Kepler-296 c | Mass-Radius* | $U(0.0660, 0.0920)$ | 0* | $U(1.34, 1.9)$ | Barclay et al. (2015) |
| | Kepler-296 d | Mass-Radius* | $U(0.0980, 0.1380)$ | 0* | $U(1.77, 2.42)$ | Barclay et al. (2015) |
| | Kepler-296 e | Mass-Radius* | $U(0.1410, 0.1980)$ | 0* | $U(1.28, 1.8)$ | Barclay et al. (2015) |
| | Kepler-296 f | Mass-Radius* | $U(0.2130, 0.2980)$ | 0* | $U(1.5, 2.11)$ | Barclay et al. (2015) |
| | Kepler-299 b | Mass-Radius* | $U(0.032, 0.048)^*$ | 0* | $U(1.05, 1.59)$ | Rowe et al. (2014) |
| | Kepler-299 c | Mass-Radius* | $U(0.056, 0.084)^*$ | 0* | $U(2.02, 3.28)$ | Rowe et al. (2014) |
| | Kepler-299 d | Mass-Radius* | $U(0.0944, 0.1416)^*$ | 0* | $U(1.48, 2.24)$ | Rowe et al. (2014) |
| | Kepler-299 e | Mass-Radius* | $U(0.176, 0.264)^*$ | 0* | $U(1.48, 2.26)$ | Rowe et al. (2014) |

| | | | | | |
|--------------|------------------------------|-----------------------|-----------------|-------------------|------------------------|
| Kepler-306 b | Mass-Radius* | $U(0.04, 0.06)^*$ | 0* | $U(1.42, 1.62)$ | Rowe et al. (2014) |
| Kepler-306 c | Mass-Radius* | $U(0.0536, 0.0804)^*$ | 0* | $U(2.16, 2.54)$ | Rowe et al. (2014) |
| Kepler-306 d | Mass-Radius* | $U(0.096, 0.144)^*$ | 0* | $U(2.23, 2.71)$ | Rowe et al. (2014) |
| Kepler-306 e | Mass-Radius* | $U(0.1816, 0.2724)^*$ | 0* | $U(2.12, 2.42)$ | Rowe et al. (2014) |
| Kepler-32 b | Mass-Radius* | $U(0.0104, 0.0156)^*$ | 0* | $U(0.75, 0.89)$ | Fabrycky et al. (2012) |
| Kepler-32 c | Mass-Radius* | $U(0.0264, 0.0396)^*$ | 0* | $U(1.4, 1.6)$ | Fabrycky et al. (2012) |
| Kepler-32 d | Mass-Radius ($M < 1303$)* | $U(0.04, 0.06)^*$ | 0* | $U(2, 2.4)$ | Fabrycky et al. (2012) |
| Kepler-32 e | Mass-Radius ($M < 158.9$)* | $U(0.072, 0.108)^*$ | 0* | $U(1.8, 2.2)$ | Fabrycky et al. (2012) |
| Kepler-32 f | Mass-Radius* | $U(0.104, 0.156)^*$ | 0* | $U(2.5, 2.9)$ | Fabrycky et al. (2012) |
| Kepler-33 b | Mass-Radius* | $U(0.0663, 0.0691)$ | 0* | $U(1.56, 1.92)$ | Lissauer et al. (2012) |
| Kepler-33 c | Mass-Radius* | $U(0.1164, 0.1214)$ | 0* | $U(2.9, 3.5)$ | Lissauer et al. (2012) |
| Kepler-33 d | Mass-Radius* | $U(0.1627, 0.1697)$ | 0* | $U(4.86, 5.84)$ | Lissauer et al. (2012) |
| Kepler-33 e | Mass-Radius* | $U(0.2093, 0.2183)$ | 0* | $U(3.64, 4.4)$ | Lissauer et al. (2012) |
| Kepler-33 f | Mass-Radius* | $U(0.2481, 0.2589)$ | 0* | $U(4.05, 4.87)$ | Lissauer et al. (2012) |
| Kepler-341 b | Mass-Radius* | $U(0.048, 0.072)^*$ | 0* | $U(0.56, 1.8)$ | Rowe et al. (2014) |
| Kepler-341 c | Mass-Radius* | $U(0.064, 0.096)^*$ | 0* | $U(0.84, 2.56)$ | Rowe et al. (2014) |
| Kepler-341 d | Mass-Radius* | $U(0.1456, 0.2184)^*$ | 0* | $U(0.91, 2.79)$ | Rowe et al. (2014) |
| Kepler-341 e | Mass-Radius* | $U(0.1936, 0.2904)^*$ | 0* | $U(0.96, 3.02)$ | Rowe et al. (2014) |
| Kepler-402 b | Mass-Radius* | $U(0.0408, 0.0612)^*$ | 0* | $U(0.98, 1.46)$ | Rowe et al. (2014) |
| Kepler-402 c | Mass-Radius* | $U(0.0544, 0.0816)^*$ | 0* | $U(1.21, 1.91)$ | Rowe et al. (2014) |
| Kepler-402 d | Mass-Radius* | $U(0.0696, 0.1044)^*$ | 0* | $U(1.11, 1.65)$ | Rowe et al. (2014) |
| Kepler-402 e | Mass-Radius* | $U(0.0816, 0.1224)^*$ | 0* | $U(1.17, 1.75)$ | Rowe et al. (2014) |
| Kepler-444 b | Mass-Radius* | $U(0.0410, 0.0426)$ | $U(0.06, 0.37)$ | $U(0.389, 0.419)$ | Campante et al. (2015) |
| Kepler-444 c | Mass-Radius* | $U(0.0479, 0.0497)$ | $U(0.16, 0.43)$ | $U(0.48, 0.518)$ | Campante et al. (2015) |
| Kepler-444 d | Mass-Radius* | $U(0.0589, 0.0611)$ | $U(0.06, 0.34)$ | $U(0.511, 0.552)$ | Campante et al. (2015) |
| Kepler-444 e | Mass-Radius* | $U(0.0683, 0.0709)$ | $U(0.03, 0.3)$ | $U(0.531, 0.563)$ | Campante et al. (2015) |
| Kepler-444 f | Mass-Radius* | $U(0.0796, 0.0826)$ | $U(0.1, 0.49)$ | $U(0.701, 0.782)$ | Campante et al. (2015) |
| Kepler-62 b | Mass-Radius ($M < 9$)* | $U(0.0548, 0.0558)$ | 0* | $U(1.27, 1.35)$ | Borucki et al. (2013) |
| Kepler-62 c | Mass-Radius ($M < 4$)* | $U(0.0920, 0.0938)$ | 0* | $U(0.51, 0.57)$ | Borucki et al. (2013) |
| Kepler-62 d | Mass-Radius ($M < 14$)* | $U(0.1190, 0.1210)$ | 0* | $U(1.88, 2.02)$ | Borucki et al. (2013) |
| Kepler-62 e | Mass-Radius ($M < 36$)* | $U(0.4230, 0.4310)$ | 0* | $U(1.56, 1.66)$ | Borucki et al. (2013) |

| | | | | | |
|--------------|---------------------------|-----------------------|----------------------|-------------------|-----------------------------|
| Kepler-62 f | Mass-Radius ($M < 35$)* | $U(0.7110, 0.7250)$ | 0* | $U(1.34, 1.48)$ | Borucki et al. (2013) |
| Kepler-79 b | $U(4.9, 18.3)$ | $U(0.1150, 0.1190)$ | $U(0.009, 0.027)$ | N/A | Jontof-Hutter et al. (2014) |
| Kepler-79 c | $U(3.6, 7.8)$ | $U(0.1840, 0.1890)$ | $U(0.009, 0.057)$ | N/A | Jontof-Hutter et al. (2014) |
| Kepler-79 d | $U(4.4, 8.1)$ | $U(0.2830, 0.2910)$ | $U(0.002, 0.084)$ | N/A | Jontof-Hutter et al. (2014) |
| Kepler-79 e | $U(3, 5.3)$ | $U(0.3810, 0.3910)$ | $U(0.007, 0.056)$ | N/A | Jontof-Hutter et al. (2014) |
| Kepler-82 b | Mass-Radius* | $U(0.0272, 0.0408)^*$ | 0* | $U(1.5, 2.04)$ | Freudenthal et al. (2019) |
| Kepler-82 c | Mass-Radius* | $U(0.0504, 0.0756)^*$ | 0* | $U(2.1, 2.84)$ | Freudenthal et al. (2019) |
| Kepler-82 d | $U(11.28, 13.11)$ | $U(0.1663, 0.1703)$ | $U(0.00313, 0.0052)$ | N/A | Rowe et al. (2014) |
| Kepler-82 e | $U(12.7, 15.2)$ | $U(0.2594, 0.2658)$ | $U(0.0052, 0.0086)$ | N/A | Rowe et al. (2014) |
| TOI-1246 b | $U(7, 9.2)$ | $U(0.0470, 0.0510)$ | 0* | N/A | Turtelboom et al. (2022) |
| TOI-1246 c | $U(7.6, 10)$ | $U(0.0590, 0.0630)$ | 0* | N/A | Turtelboom et al. (2022) |
| TOI-1246 d | $U(3.6, 7)$ | $U(0.1270, 0.1350)$ | 0* | N/A | Turtelboom et al. (2022) |
| TOI-1246 e | $U(12.5, 17.1)$ | $U(0.2040, 0.2180)$ | 0* | N/A | Turtelboom et al. (2022) |
| TOI-178 b | $U(1.06, 1.89)$ | $U(0.0253, 0.0268)$ | 0* | N/A | Leleu et al. (2021) |
| TOI-178 c | $U(4.09, 5.32)$ | $U(0.0359, 0.0381)$ | 0* | N/A | Leleu et al. (2021) |
| TOI-178 d | $U(1.98, 3.81)$ | $U(0.0574, 0.0610)$ | 0* | N/A | Leleu et al. (2021) |
| TOI-178 e | $U(2.92, 5.11)$ | $U(0.0759, 0.0806)$ | 0* | N/A | Leleu et al. (2021) |
| TOI-178 f | $U(6.2, 9.39)$ | $U(0.1008, 0.1070)$ | 0* | N/A | Leleu et al. (2021) |
| TOI-178 g | $U(2.32, 5.25)$ | $U(0.1236, 0.1313)$ | 0* | N/A | Leleu et al. (2021) |
| TOI-561 b | $U(1.77, 2.23)$ | $U(0.0105, 0.0107)$ | 0* | N/A | Lacedelli et al. (2022) |
| TOI-561 c | $U(4.71, 6.08)$ | $U(0.0875, 0.0893)$ | $U(0.009, 0.065)$ | N/A | Lacedelli et al. (2022) |
| TOI-561 d | $U(12.3, 14.2)$ | $U(0.1560, 0.1600)$ | $U(0.074, 0.176)$ | N/A | Lacedelli et al. (2022) |
| TOI-561 e | $U(11.2, 14)$ | $U(0.3250, 0.3310)$ | $U(0.029, 0.137)$ | N/A | Lacedelli et al. (2022) |
| TOI-700 b | Mass-Radius* | $U(0.0666, 0.0688)$ | $U(0.021, 0.168)$ | $U(0.865, 0.967)$ | Gilbert et al. (2023) |
| TOI-700 c | Mass-Radius* | $U(0.0914, 0.0944)$ | $U(0.019, 0.138)$ | $U(2.47, 2.74)$ | Gilbert et al. (2023) |
| TOI-700 d | Mass-Radius* | $U(0.1318, 0.1362)$ | $U(0.017, 0.116)$ | $U(0.878, 1.042)$ | Gilbert et al. (2023) |
| TOI-700 e | Mass-Radius* | $U(0.1606, 0.1660)$ | $U(0.012, 0.087)$ | $U(1.019, 1.132)$ | Gilbert et al. (2023) |
| TRAPPIST-1 b | $U(1.305, 1.443)$ | $U(0.0114, 0.0116)$ | 0* | N/A | Agol et al. (2021) |
| TRAPPIST-1 c | $U(1.252, 1.364)$ | $U(0.0157, 0.0159)$ | 0* | N/A | Agol et al. (2021) |
| TRAPPIST-1 d | $U(0.376, 0.4)$ | $U(0.0221, 0.0225)$ | 0* | N/A | Agol et al. (2021) |
| TRAPPIST-1 e | $U(0.67, 0.714)$ | $U(0.0268, 0.0318)$ | 0* | N/A | Agol et al. (2021) |

| | | | | | |
|--------------|-------------------|---------------------|----|------------------|---------------------|
| TRAPPIST-1 f | $U(1.008, 1.07)$ | $U(0.0382, 0.0388)$ | 0* | N/A | Agol et al. (2021) |
| TRAPPIST-1 g | $U(1.283, 1.359)$ | $U(0.0464, 0.0472)$ | 0* | N/A | Agol et al. (2021) |
| TRAPPIST-1 h | $U(0.306, 0.346)$ | $U(0.0614, 0.0624)$ | 0* | N/A | Agol et al. (2021) |
| V1298 Tau b | Mass-Radius* | $U(0.0812, 0.0838)$ | 0* | $U(5.27, 5.95)$ | David et al. (2019) |
| V1298 Tau c | Mass-Radius* | $U(0.1066, 0.1100)$ | 0* | $U(6.01, 6.86)$ | David et al. (2019) |
| V1298 Tau d | Mass-Radius* | $U(0.1662, 0.1714)$ | 0* | $U(9.74, 10.85)$ | David et al. (2019) |
| V1298 Tau e | Mass-Radius* | $U(0.2420, 0.4900)$ | 0* | $U(8.02, 9.58)$ | David et al. (2019) |